VATNAJÖKULL:
Mass balance, meltwater drainage and surface velocity of the glacial year 2019_20

Institute of Earth Sciences
University of Iceland
and
National Power Company

Finnur Pálsson
Andri Gunnarsson
Hlynur Skagfjörð Pálsson
Sveinbjörn Steinþórsson

RH-07-20

Contents:

Figures:

1. **INTRODUCTION**

In 1992 (glacial year 1991_92) a program of surface mass balance measurements was started for Vatnajökull by the Science Institute University of Iceland (now Institute of Earth Sciences, IES) in collaboration with the National Power Company (NPC). For the first year the program was limited to the western part of the glacier, but then expanded to include the northern outlets as well. In 1996 this study was further expanded to include southern outlets, with support from The European Union (Framework IV - Environment and Climate, TEMBA project 1996-1997). This program was extended 1998–2000 with further support from EU (Framework IV - Environment and Climate, ICEMASS project, 1998-2000). In 2000-2002 NPC and IES continued the program. In 2003-2005 IES participated in a multinational research project, which was financially supported by The European Union (EVK2-CT-2002-00152 SPICE). IES was responsible for obtaining data sets for calibration of models of the mass balance and dynamics of Vatnajökull. This work was also supported by The National Power Company of Iceland and The National Road Authority, and was a continuation of the TEMBA-project of 1996-97 and ICEMASS project 1998-2001.
Since then IES and NPC have continued a similar program. Mass balance measurements on the southeast outlet Breiðamerkurjökull is financially supported by the National Road Authority.
The aim of the collaborative work of NPC and IES is to improve understanding of the mass balance and melt water runoff from glaciers. This work in combination with energy balance measurements by NPC and IES on Vatnajökull will is used for calibration of models of the surface energy and mass balance of Vatnajökull.
This report describes the field measurements, mass balance, melt water runoff and GPS survey, for the glaciological year 2019_20.

2. DIARY

March 27-28: installation of melt wires, maintenance of AWSs on Breiðamerkurjökull.
April 28 - May 4: measurements of the winter balance, setup of AWSs.
August 13; October 8 - 13 and November 25: summer balance measurements; maintenance of AWSs on Breiðamerkurjökull.

In all expeditions and short visits to the glacier the locations of mass balance stakes were measured with Kinematic GPS (or fast static GPS) for surface velocity calculation.

The following members of staff of the Institute of Earth Sciences, University of Iceland, carried out the fieldwork on Vatnajökull: Finnur Pálsson, Sveinbjörn Steinþórsson with Andri Gunnarsson and Gestur Jónsson (National Power Company), Hlynur Skagfjörð Pálsson (Reykjavík Rescue Team), Haraldur Mímir Bjarnason (Neyðarlínan), and Jón Yngvi Gylfason Mountain Guide.

3. MASS BALANCE MEASUREMENTS

The purpose of the mass balance measurements is to describe the temporal and spatial distribution of the components of the mass balance. The mean annual values of the components and their variation from year to year are analyzed and related to meteoro-logical conditions and climatic variability. The results are used in studies of changes in the glacier volume, estimates of meltwater contribution to glacial rivers, mass balance modeling, evaluation of altitudinal and regional variations of mass balance in response to climatic variations, and to assess the hydrometeorological and dynamic response of the ice cap to climate change.

The mass balance was determined by a stratigraphic method, measuring changes in thickness and density relative to the summer surface. The winter balance was estimated by drilling ice cores through the winter layer in the spring. Ablation was monitored from markers; snow stakes were put up on the glacier and wires were drilled down in the ablation area. The summer balance was measured in the autumn.

3.1 Methods

Measurements of the surface mass balance on a large ice cap like Vatnajökull are impractical in terms of cost with conventional techniques and sampling density that are typically used on small glaciers. The spatial variability of the mass balance may, however, be predictable on the flat large outlets of such an ice cap given data on several profiles extending over the elevation range of the glacier. The precipitation generally increases with elevation and decreases with the distance from the coast, but both the distribution of snowfall and redistribution of snow by drift depend on the prevailing wind direction during the winter. The summer melting depends mainly on the altitude and the albedo of the glacier surface. Therefore, we have used observations along a limited number of flowlines, which span the elevation ranges of the outlets to assess aerial estimates of surface mass balance. Each profile describes the variation with elevation, but together they also describe the lateral variation of the mass balance. Recently, modern over-snow vehicles and helicopters have allowed fast traverses to ensure successful fieldwork in spite of frequently poor weather conditions. The error for individual point measurement is estimated ~30 cm_{we} for both summer and winter balance. The error for the glacier wide specific mass balance, based on area integral of mass balance, is however considered smaller, since the error for individual survey sites is independent.

The winter mass balance (b_w) is defined as the mass of snow accumulated during the winter months, the summer balance (b_s) is the mass balance during the summer, and the net balance (b_n) is defined as their sum. The specific mass balance is expressed in terms of the equivalent thickness of water. All mass balance components apply to a time interval between given measurement dates, which are not fixed from one year to another. The dates in the autumn are separated by approximately one calendar year, which roughly coincides with the glaciological year defined as October 1st to September 30th. Snow cores are drilled in April-May through the winter layer and profiles of the density are measured. The summer balance is derived in the autumn from measurements of the changes in the snow core density during the summer in the accumulation area and from

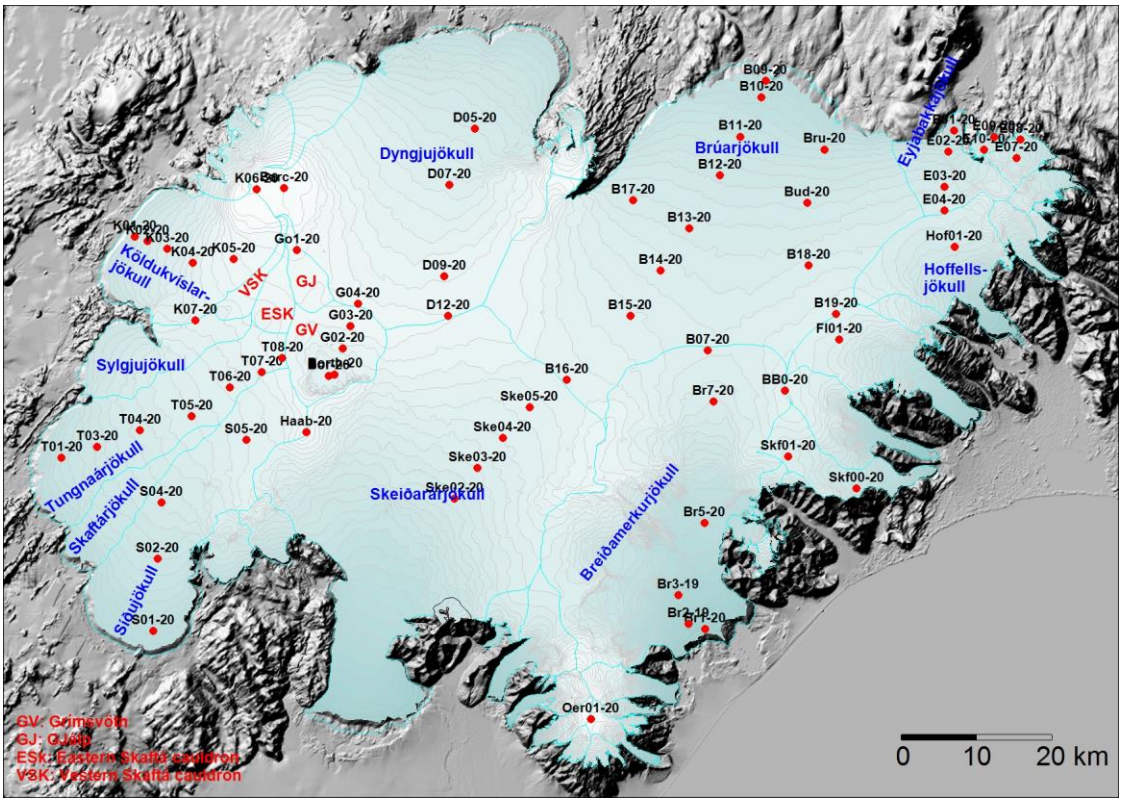

Figure 1. Outlets of Vatnajökull and location of mass balance survey sites 2019_20.

readings at stakes and wires drilled into the ice in the ablation areas.

Digital maps are created for winter, summer and net balance for the whole ice cap based on the in-situ measurements. The mass balance is calculated over both the ice and water drainage basins. The summer balance over the water basin is an estimate of meltwater contribution to rivers and groundwater storage. This estimate, however, does not include precipitation that falls as rain on the glacier or snow, which falls and melts during the summer. As conventional for the north hemisphere we define the glaciological year from the start of October to the end of September next year and the period draining meltwater from the glacier during the summer from start of June through September. It would be misleading to include May in the summer period because runoff from the glacier melt in May is delayed due to refreezing during the elimination of the frost in the surface layer.

3.2 Results of mass balance measurements.

Winter mass balance measurements were done at 67 sites in spring 2020 (Fig. 1). The specific mass balance at individual sites is shown in Fig. 2. Most survey sites are on approximate central flow lines at individual outlets. The specific mass balance along the flow lines is given in Fig 3. for the glacier outlets: Síðujökull, Tungnaárjökull, Köldukvíslarjökull, Dyngjujökull, Brúarjökull (west and east), Eyjabakkajökull, Breiðamerkurjökull, SE-Vatnajökull, Skeiðarárjökull accumulation zone and the ice catchment of Grímsvötn.

Digital maps for winter, summer and net balance are shown in Figure 4. The mass balance of individual outlet is discussed in the following subsections.

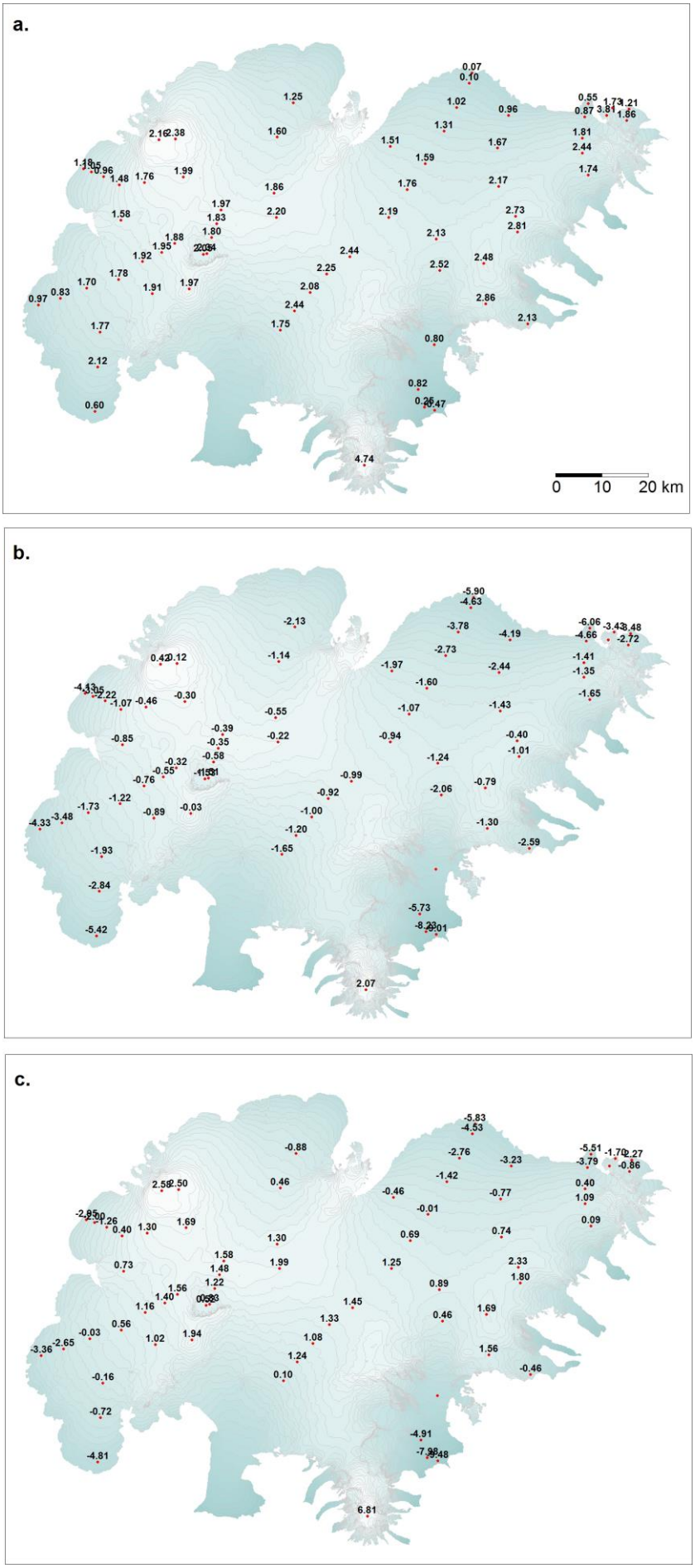

Figure 2. Maps showing point values of specific surface mass balance in m water equivalent (m_{we}), 2019_20. a. winter, b. summer, c. net balance.

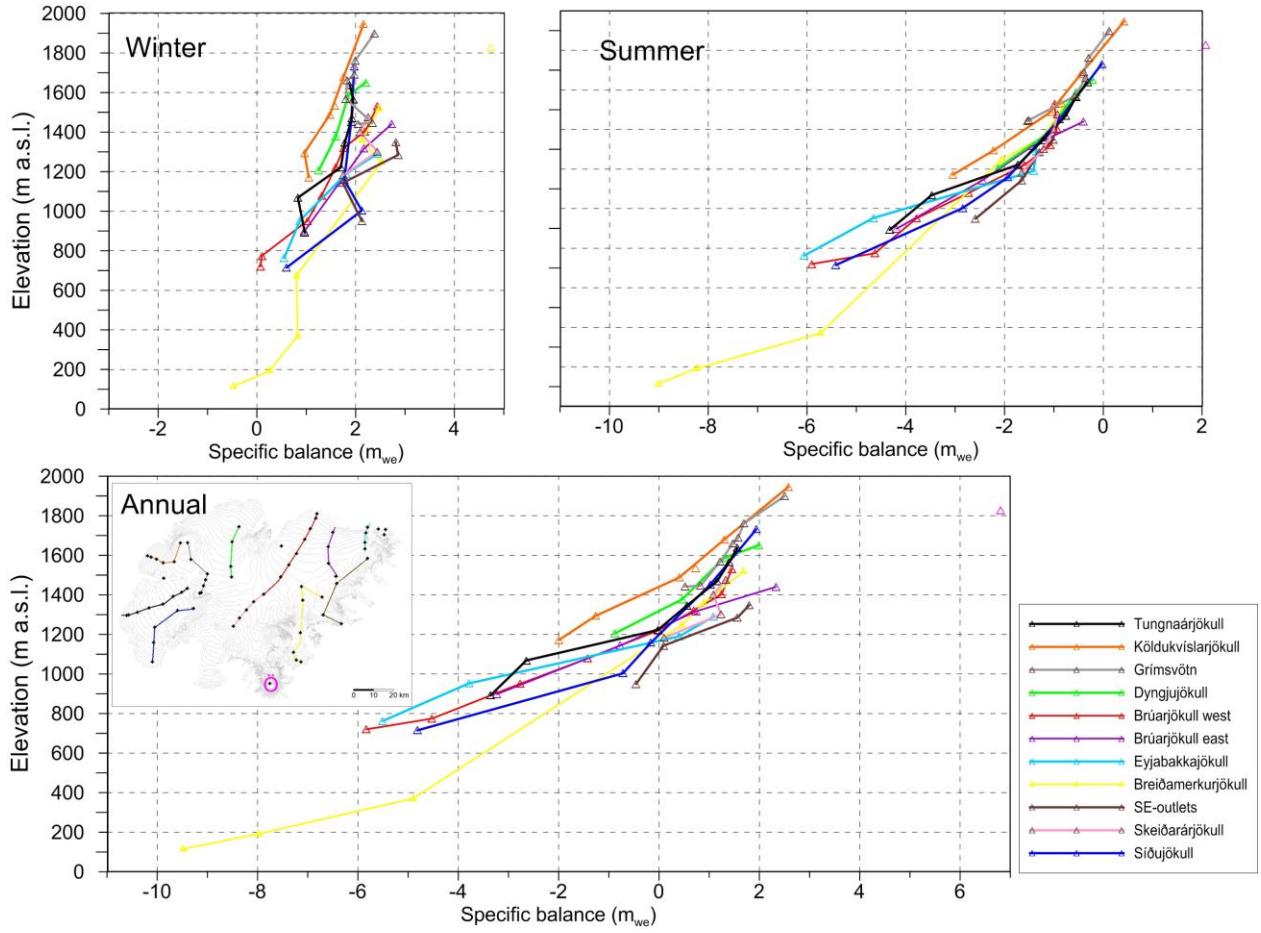

Figure 3. a. Specific mass balance (m_{we}), at survey sites along all mass balance profiles 2019_20.

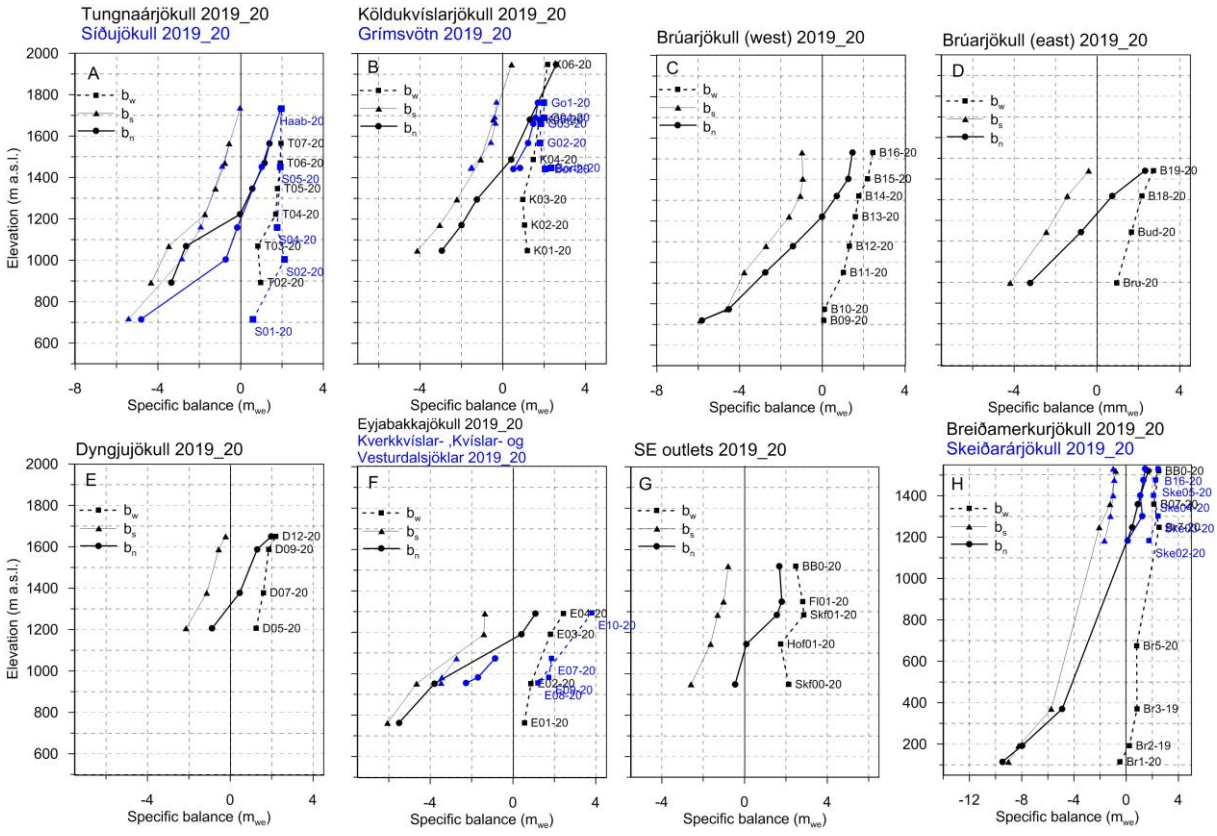

Figure 3. b. Specific point mass balance (m_{we}) 2019_20 as a function of elevation on central flow lines on Vatnajökull outlets.

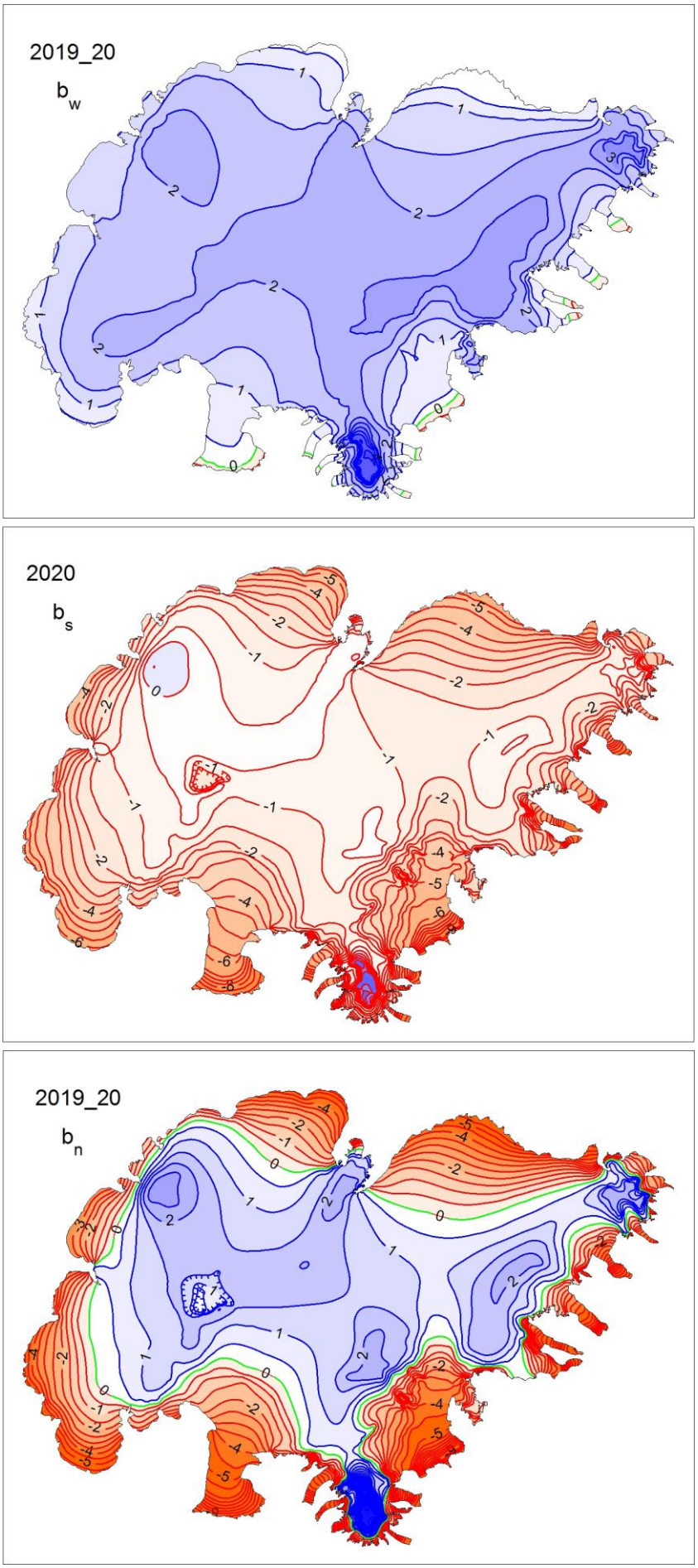

Figure 4. Specific mass balance (m_{we}) maps of Vatnajökull 2019_20. Top: winter, Centre: summer, Bottom: net balance.

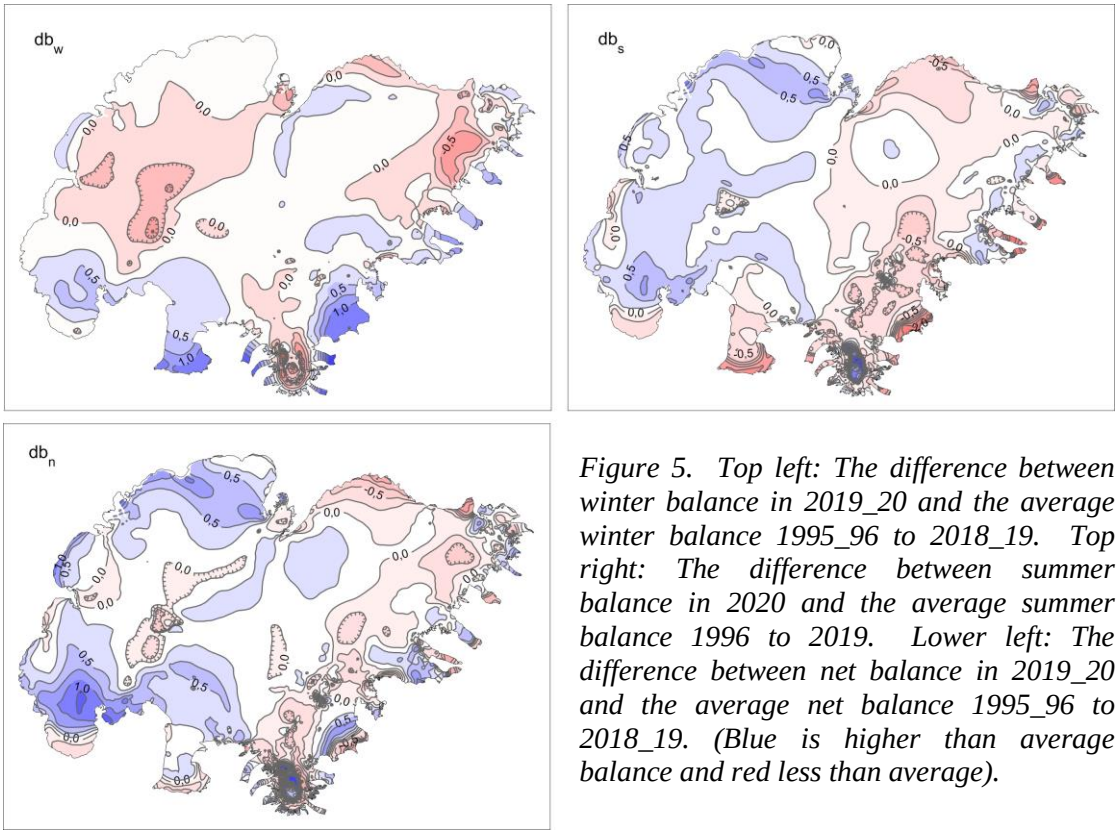

Figure 5. Top left: The difference between winter balance in 2019_20 and the average winter balance 1995_96 to 2018_19. Top right: The difference between summer balance in 2020 and the average summer balance 1996 to 2019. Lower left: The difference between net balance in 2019_20 and the average net balance 1995_96 to 2018_19. (Blue is higher than average balance and red less than average).

A surface DEM is needed for surface area distribution and delineation of ice divides for individual outlets and catchments. The currently used surface DEM is mostly based on SPOT5 satellite images in 2010*, and partly from LiDAR survey 2010 -11 and -12 (**Jóhannesson et al. 2013), but the large set of GPS profiles measured in spring 2020 was used to locally shift the older DEMs. This DEM representing the surface of 2020 but now cut to the glacier terminus of autumn 2019, of was used in all area distributions; ice and water divides were not reworked.

The weather in the autumn and first winter months 2019_20, was wet and rather warm, not much snow below ~1000 m. In latter half of winter snow collected on all except the lowest lying snouts.

Figure 5 (top left) shows that the winter accumulation is under average at all higher accumulation zones, but more than average in all the ablation zones, especially in the south and. winter melting at the low lying S-outlets much less than average.

The summer months were mostly warm and dry in the East and SE but wet and cloudy in the west. Wet cold spells of northern direction caused occasional snow fall even in July, especially onto the northern outlets.

In addition relatively little dust precipitated on the glacier, so albedo was quite high. Thick winter snow in the ablation zone of the western outlets also reduced summer melt.

*SPOT 5 HRG images were made available by the French Space Agency (CNES) through the ISIS (Incentive for the Scientific use of Images from the SPOT system) program and SPOT 5 HRS digital elevation models by the Spot Image project Planet Action (www.planet-action.org) and the SPIRIT SPOT 5 stereoscopic survey of Polar Ice.

**Jóhannesson, T., Björnsson, H., Magnússon, E., Guðmundsson, S.,Pálsson, F., Sigurðsson, O., Thorsteinsson, T., and Berthier, E.: Ice-volume changes, bias estimation of mass-balance measurements and changes in subglacial lakes derived by lidar mapping of the surface Icelandic glaciers, Ann. Glaciol., 54, 63–74, doi:10.3189/2013AoG63A422,2013.

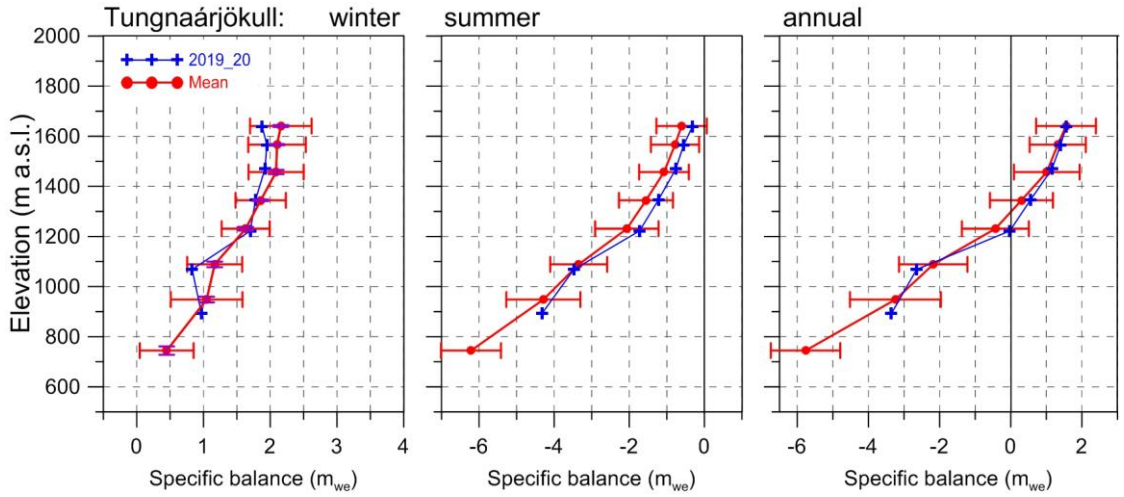

Figure 6. Mass balance at a central flow line of Tungnaárjökull 2019_20 and average mass balance 1991_92 to 2018_19 (the horizontal red lines indicate std. dev of the variability at the survey site during the survey period).

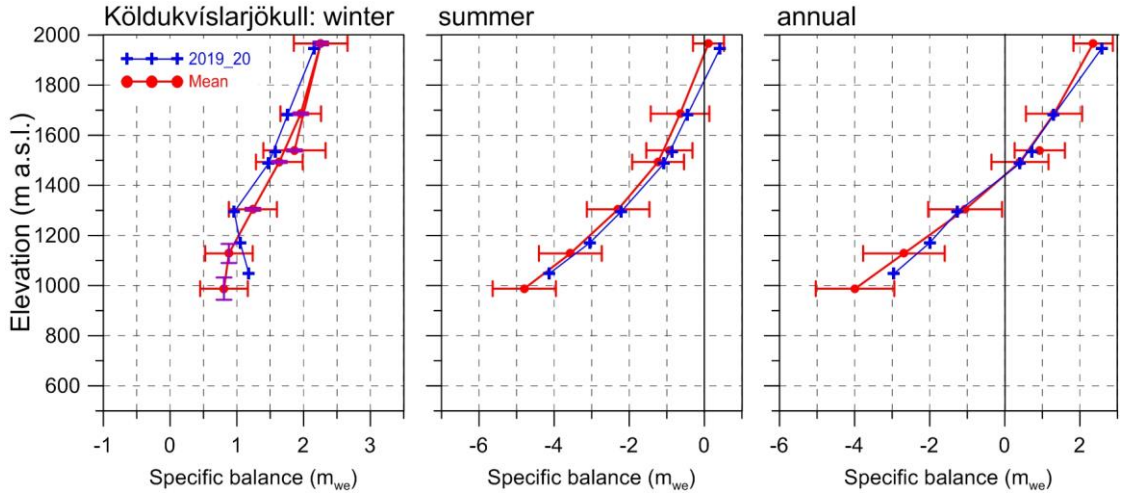

Figure 7. Mass balance at a central flow line of Köldukvíslarjökull 2019_20 and average mass balance 1991_92 to 2018_19.

3.2.1 Tungnaárjökull.

Area = 330 km^2
B_w= 0.51 km^3_{we} ; b_w = 1.53 m_{we}
B_s = -0.76 km^3_{we} ; b_s = -2.30 m_{we}
B_n = -0.25 km^3_{we} ; b_n = -1.77 m_{we}
ELA = 1225 m a.s.l. (at profile)
AAR = 50 %
(The terms are defined at the foot of this page)

Variation of mass balance along a central flow line on Tungnaárjökull is shown in Fig. 6. The winter accumulation was less than average at all survey sites except close to the ELA The total winter balance was almost 90% of average. Summer mass loss was less at all survey sites especially at the higher sites. Summer mass loss was only 70% of the average of the survey period. Similar applies to the net balance. In total the net mass loss amounted to 95% of average of the survey period. This is the 26th year out of the 29 surveyed with negative net balance on Tungnaárjökull catchment.

3.2.2 Köldukvíslarjökull

Area = 289 km^2
B_w = 0.43 km^3_{we} ; b_w = 1.48 m_{we}
B_s = -0.47 km^3_{we}; b_s = -1.63 m_{we}
B_n = -0.04 km^3_{we}; b_n = -0.15 m_{we}
ELA = 1440 m a.s.l. (at profile)
AAR = 53 %

Variation of mass balance along a central flow line on Köldukvíslarjökull

For each ice catchment basin, B_w, B_s and B_n are water equivalent volumes of winter, summer and net balance, ELA the equilibrium line altitude, and AAR is the accumulation area ratio.

is shown in Fig. 7. The winter accumulation close to average at the highest but far under average at the other, except the 2 lowest where it exceeded average by almost ~1 std. The total winter accumulation was at average. Summer mass loss was slightly less than average at all survey sites and in total 83% of the average during the survey period. In total the net mass loss was only 1/3 that of an average year of the survey period. This is the 24th year out of the 29 surveyed with negative net balance.

3.2.3 Dyngjujökull

Area = 1039 km^2
B_w = 1.67 km^3_{we} ; b_w= 1.61 m_{we}
B_s = -1.45 km^3_{we} ; b_s = -1.39 m_{we}
B_n = 0.22 km^3_{we} ; b_n = 0.22 m_{we}
ELA = 1320 m a.s.l. (at profile)
AAR = 68 %

Variation of mass balance along a flow line on Dyngjujökull is shown on Fig. 8. Mass balance is not measured at the lowest elevations, but assumed to be correlated (as a function of elevation) to that of Brúarjökull and Köldukvíslarjökull. Inspection of the winter Modis satellite images suggests that, at the glacier snout, snow cover was very thin below. The site measurements show less than average snow accumulation in the upper part of the accumulation zone, but slightly over average at the lower two. The total winter accumulation is estimated almost at the average of the survey period.

Summer mass loss was slightly less than average over the survey period at all survey sites. The total mass loss was ~85% of an average summer.

The total net balance was positive by 0.22 m_{we} while the average for Dyngjujökull is only slightly negative (-0.04 m_{we}).

Dyngjujökull has often had mass balance close to zero, and the net balance has been estimated positive in at least 11 years of the almost three decade period of almost continuous mass loss for Vatnajökull as a whole.

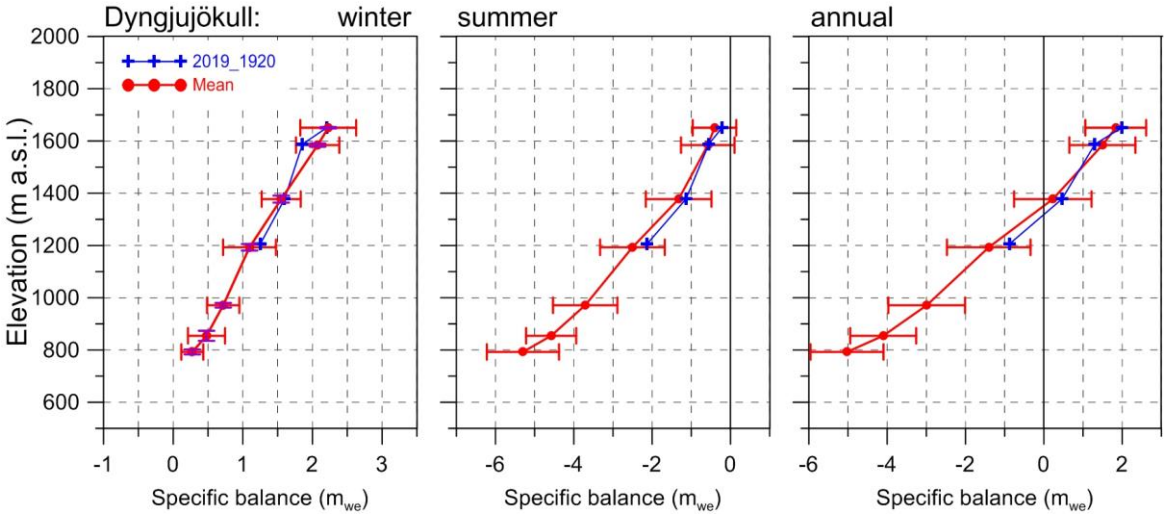

Figure 8. Mass balance at a central flow line on Dyngjujökull 2019_20 and average mass balance 1991_92 to 2018_19 (except 1998_99 – 2003_04 at all but the top elevation).

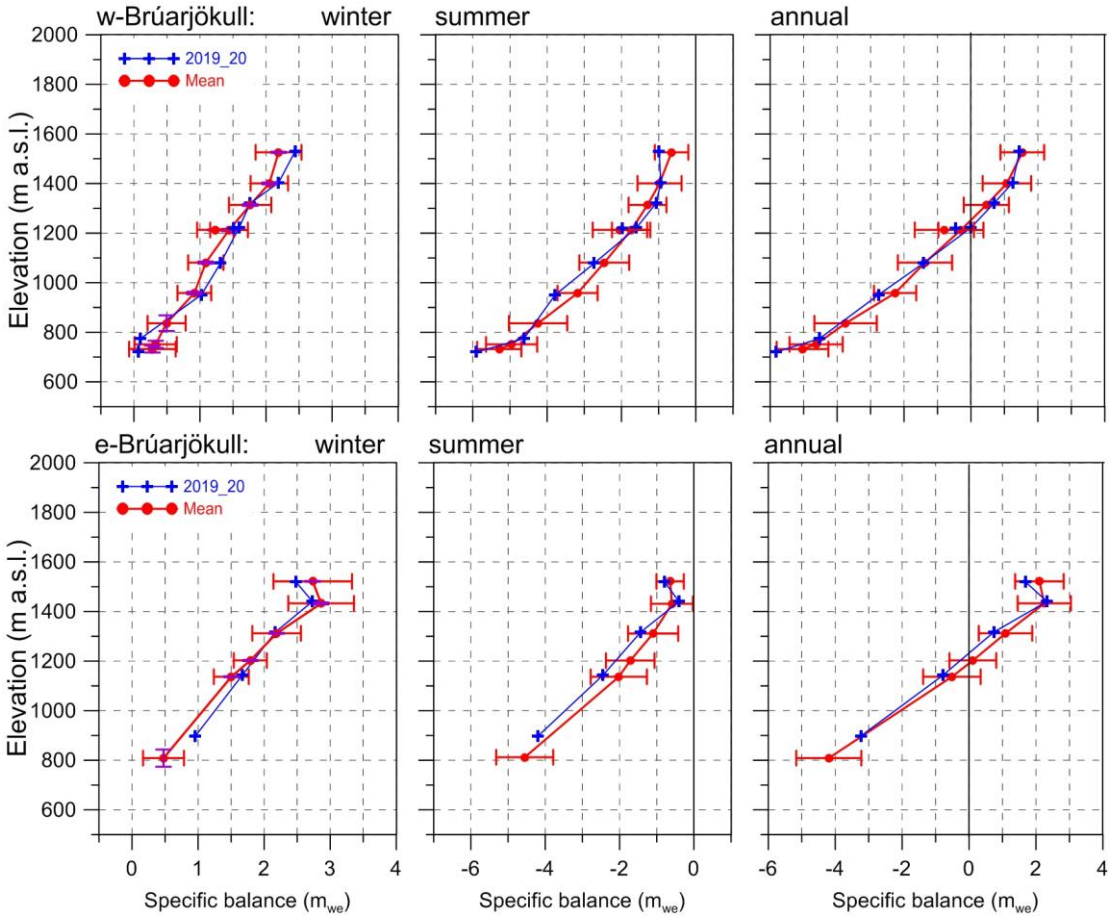

Figure 9. Mass balance at two flow lines on Brúarjökull 2019_20 and average mass balance 1992_93 to 2018_19.

3.2.4 Brúarjökull

Area = 1500 km^2
B_w = 2.61 km^3_{we} ; b_w = 1.75 m_{we}
B_s = -2.87 km^3_{we}; b_s = -1.92 m_{we}
B_n = -0.26 km^3_{we}; b_n = -0.17 m_{we}
ELA = 1220 m a.s.l. (western flow line)
ELA = 1230 m a.s.l. (eastern flow line)
AAR = 60 %

Variation of mass balance along two flow lines on Brúarjökull is shown on Fig. 9. At the western flow line accumulation was over average, except the lowest two. At the eastern line accumulation was lower than average at the highest sites, Breiðabunga, which is most prone to precipitation from eastern wind directions. In the ablation zone snow collection was over the average. The winter accumulation was in total about 10% higher than average. Summer mass loss was close to average, except in the mid elevation range, probably due to snowfall in summer. In total the mass loss in summer was exceeded the average by 1% (not significant). The net balance was close to average at most sites. In total the net balance was negative by -0.17 m_{we}, or about 60% of the average mass loss of the survey period.
During the survey period, there have been 8 years of positive balance and 20 years with negative net balance.

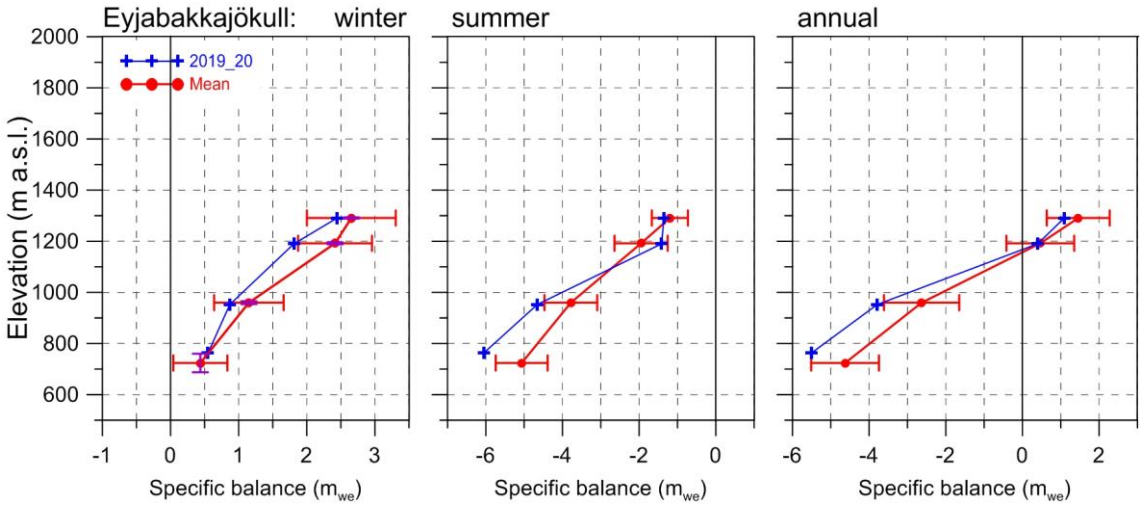

Figure 10. Mass balance at a central flow line of Eyjabakkajökull 2019_20 and average mass balance 1995_96 to 2018_19.

3.2.5 Eyjabakkajökull

Area = 106 km^2
B_w= 0.19 km^3_{we}; b_w = 1.80 m_{we}
B_s = -0.27 km^3_{we}; b_s = -2.58 m_{we}
B_n = -0.82 km^3_{we}; b_n = -0.78 m_{we}
ELA = 1165 m a.s.l. (at profile)
AAR = 47 %

Variation of mass balance along a central flow line on Eyjabakkajökull is shown on Fig. 10. Accumulation was less than average at all sites, especially the upper ones, just as on E Brúarjökull. The total winter was at average of the survey period (99%). Summer mass loss was by far more than average the lower sites, but much less than average close to average ELA (probably due to summer snowfall). The total summer mass loss was about 96% of the average. The net balance was negative by ~91% of the average since of the survey period, and has been negative for all but 3 years of the 25 years of survey.

3.2.6 Breiðamerkurjökull

Area = 925 km^2
B_w = 1.70 km^3_{we}; b_w = 1.84 m_{we}
B_s = -2.57 km^3_{we}; b_s = -2.78 m_{we}
B_n = -0.87 km^3_{we}; b_n= -0.94 m_{we}
ELA = 1185 m a.s.l. (at profile)
AAR = 51
Variation of mass balance along a central flow line on Breiðamerkurjökull is shown on Fig. 11.
Winter accumulation was well over

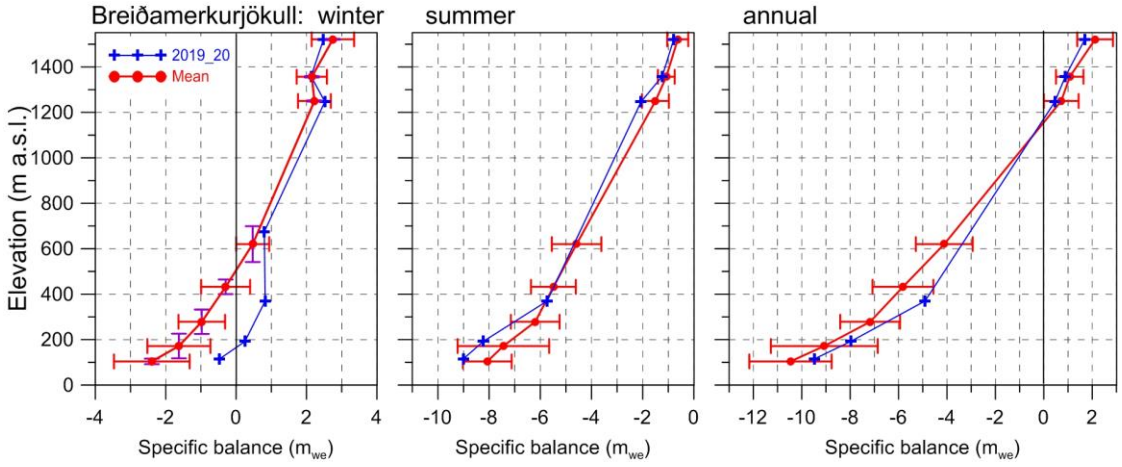

Figure 11. Mass balance at a central flow line of Breiðamerkurjökull 2019_20 and average mass balance 1995_96 to 2018_19.

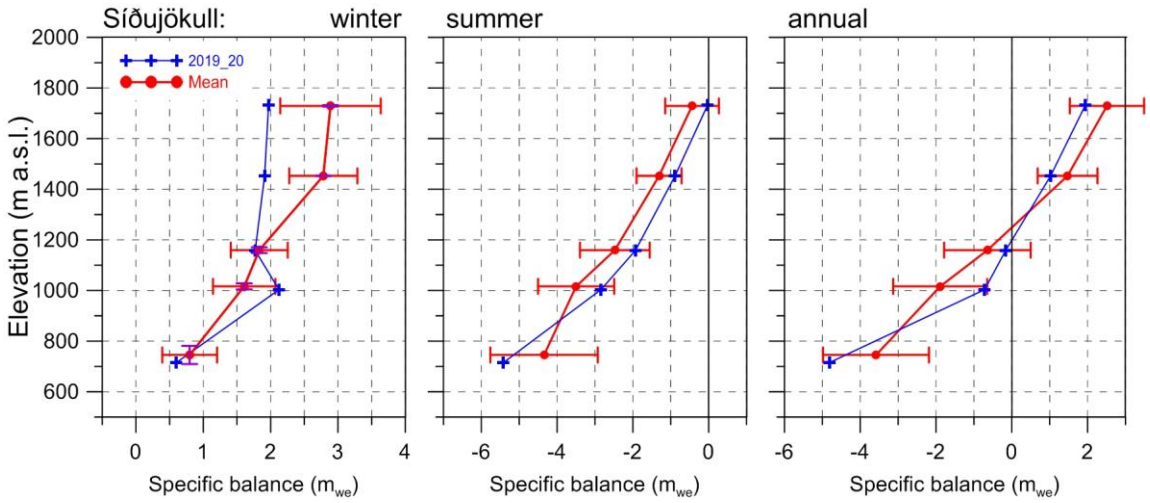

Figure 12. Mass balance at a central flow line of Síðujökull 2019_20 and average mass balance 2004_05 to 2018_19.

average at the survey sites in the accumulation zone. At the sites in the ablation zone mass loss in winter was 2 std. less than average sites. The total winter balance was 24% higher than in an average winter of the survey period. Summer mass loss was close to average in the accumulation zone, but more than 1 std. over average in the lower ablation zone. The total summer mass loss was close to 7% more than average during the survey period. The net mass loss was almost 3% more than in an average year.

In addition to mass loss due to surface melt Breiðamerkurjökull loses in the order of 0.5 km^3 annually via calving into the marginal lake Jökulsárlón; this mass loss is not accounted for here.

3.2.7 Síðujökull

Area = 410 km^2
B_w= 0.69 km^3_{we}; b_w = 1.68 m_{we}
B_s = -1.04 km^3_{we}; b_s = -2.53 m_{we}
B_n = -0.35 km^3_{we}; b_n= -0.84 m_{we}
ELA = 1200 m a.s.l. (at profile)
AAR = 52 %

Variation of mass balance along a central flow line on Síðujökull is shown in Fig. 12. The distribution of snow was very unusual; far under average in the accumulation zone but

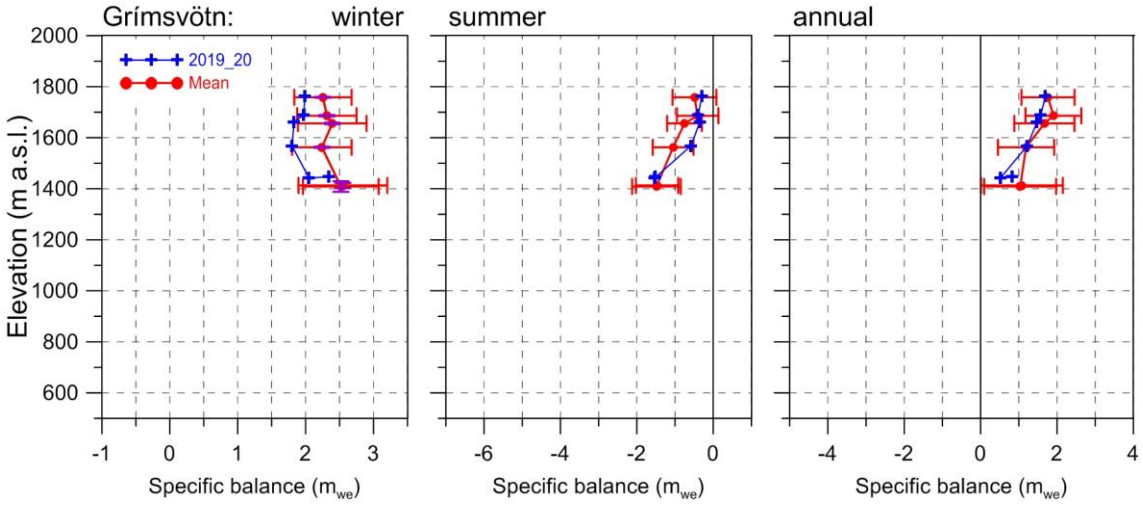

Figure 13. Mass balance at a flow line towards Grímsvötn 2019_20 and average mass balance 1991_92 to 2018_19.

far over average in the mid ablation zone. The total winter balance was ~4% over the average (since 2004_05). Summer mass loss was about 1/2 std. less than average at all sites except the lowest, and the total summer mass loss was ~86% more of the average during the survey period. Net mass loss was ~65% of the average of the 16 year survey period (only in 2014_2015 the net balance was positive).

3.2.6 Grímsvötn-Gjálp

Area = 174 km^2
B_w = 0.27 km^3_{we}; b_w = 2.00 m_{we}
B_s = -0.10 km^3_{we}; b_s = -0.71 m_{we}
B_n = 0.17 km^3_{we}; b_n= 1.29 m_{we}

Variation of mass balance at sites close to a flow line from Bárðarbunga towards Grímsvötn center is shown in Fig. 13. Snow accumulation was almost 1 std. less than average at all survey sites, and total winter accumulation only 86% the average. Summer mass loss was less than average at all but lowest sites; total summer mass loss ~87% of the average. Net balance was positive as almost always, by 85% of the average. In addition to surface mass loss in summer geothermal melt in the Grímsvötn area is on the order of 0,2 km^3 annually, this is not accounted for here.

3.3 The mass balance record for Vatnajökull.

From the digital mb maps (Fig. 4) the glacier wide volumes of winter, summer and net balances for Vatnajökull (and selected outlets) have been calculated by integration and are as follows:
B_w = 13.57 km^3_{we} ; b_w = 1.75 m_{we}
B_s = -15.94 km^3_{we} ; b_s = -2.05 m_{we}
B_n = -2.37 km^3_{we} ; b_n = -0.30 m_{we}
AAR = 59%; Area = 7770 km^2

(balance values as a function of elevation are tabulated in appendix D) The weather in the autumn and first winter months 2018_19, was wet and rather warm, not much snowfall below ~1000 m. The latter half of the winter was colder and with periods of SW wind. The summer months were mostly warm and dry in the East and SE but wet and cloudy in the west. Wet cold spells of northern direction caused occasional snow fall even in July, especially onto the northern outlets.
In addition relatively little dust precipitated on the glacier, so albedo was quite high. Thick winter snow in the ablation zone of the SW outlets also reduced summer melt.
The total winter balance was ~10%

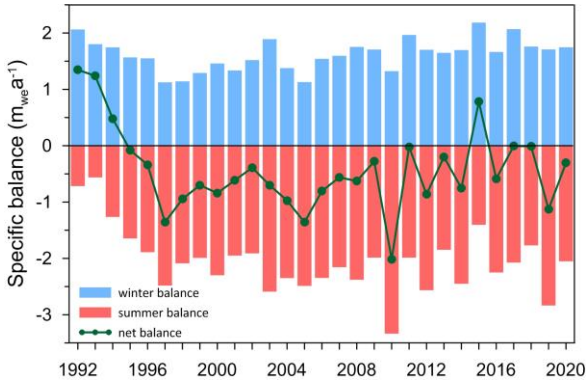

Figure 14. Specific mass balance record for Vatnajökull 1991_92 – 2019_20.

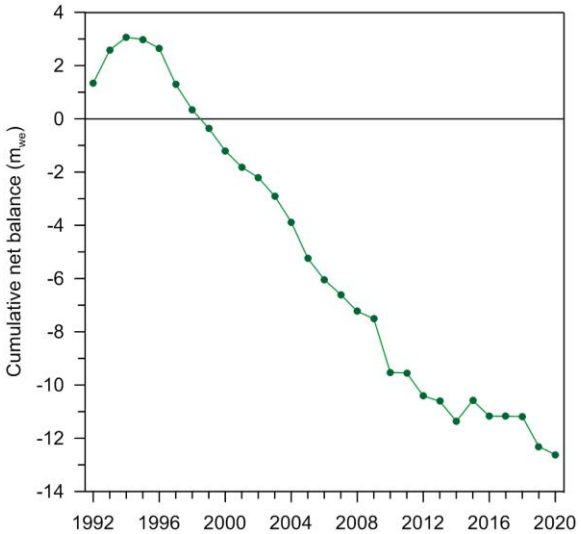

Figure 15. Cumulative specific mass balance of Vatnajökull 1991_92 – 2019_20.

higher than average (over the observation period from 1991_92, Fig. 14). The zero mass balance mass turnover for Vatnajökull (current topography) is close to 13.5 km^3_{we} (1.7 m_{we}) and the winter balance 2019_20 is ~3% higher (the zero mass turnover is estimated from the zero bn crossover when b_w, and b_s of the survey period are plotted against b_n).

The total summer mass loss was ~93% of the average since 1995 (almost exactly the average since 1992). As mentioned above, zero mass balance turnover for Vatnajökull (current topography) is close to 13.5 km^3_{we} (1,7 m_{we}), the summer mass loss 2020 was 15.94 km^3_{we} or ~18 % more loss than the zero balance mass turnover. The annual balance is negative by only 50% of the average since 1994_95 more than average (69% since 1991_92). The net balance has been negative since 1994_95 (except for 2014_15). After a short period of positive and close to zero mass

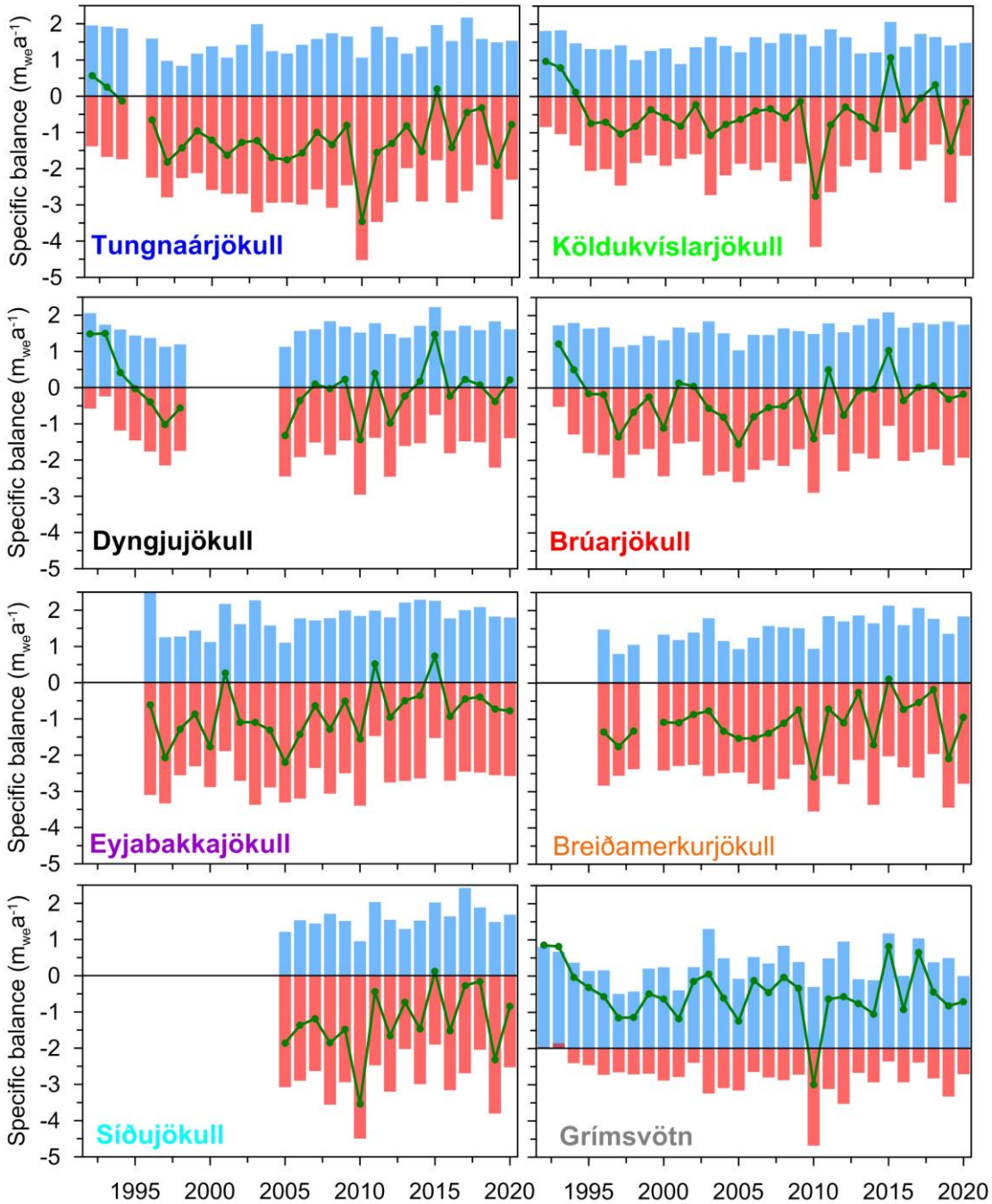

Figure 16. Specific mass balance record for Vatnajökull outlets 1991_92-2019_20.

balance, last (2018_19) year is comparable to the 20 year period of high mass loss, but the current less so.

The variability of the winter balance (Fig. 16) is by far more prominent for the outlets closest to sea. That part of the glacier receives precipitation from all south and east wind directions, and thus has high snow accumulation in winters when the paths of the North Atlantic low pressure systems are just south and east of Iceland.

During the period of high net mass loss since 1994_95, the northern outlets have had several years of close to zero and positive mass balance.

The cumulative net balance curves for the outlets of Vatnajökull in Fig. 17 show that all outlets have been losing mass since 1994_95. The slope for mass loss is about 0.7 $m_{we}a^{-1}$ for the northern outlets but 1.5 $m_{we}a^{-1}$ for the south and western outlets.

In Fig. 18 the relation of the annual net balance to the accumulation area ratio (AAR) and equilibrium line altitude (ELA) is shown for different outlets over the survey period. The b_n-AAR gradient is similar for all outlets, about 0.5 m_{we} for 10% change in AAR. The zero-balance AAR varies for different outlets in the range 60-65%, similar for all outlets except for the southern outlet Breiðamerkurjökull. Breiðamerkurjökull is far from equilibrium, the ablation area is too large. A large part of the outlet has carved 200-300 m deep through into the former sediment bed, and the surface and bed elevation has lowered accordingly. Similarly, the zero-balance ELA varies from about 1000-1100 m a.s.l. for the southern outlets to 1400 m a.s.l. for the NW outlets. The b_n-ELA slope is similar for all outlets -0.7 m_{we} per 100 m, except Eyjabakkajökull with a slope of -1.0 m_{we} per 100 m.

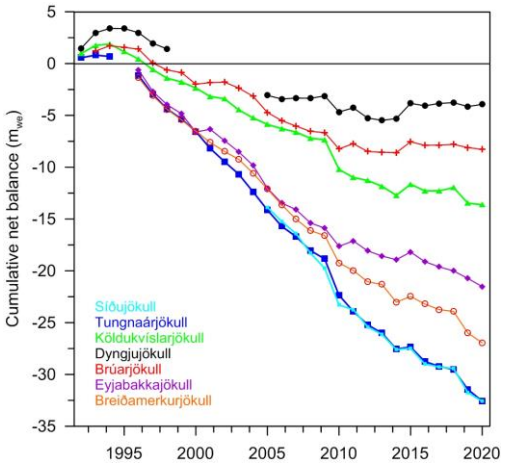

Figure 17. Cumulative specific surface mass balance for several of Vatnajökull outlets 1991_92 – 2019_20.

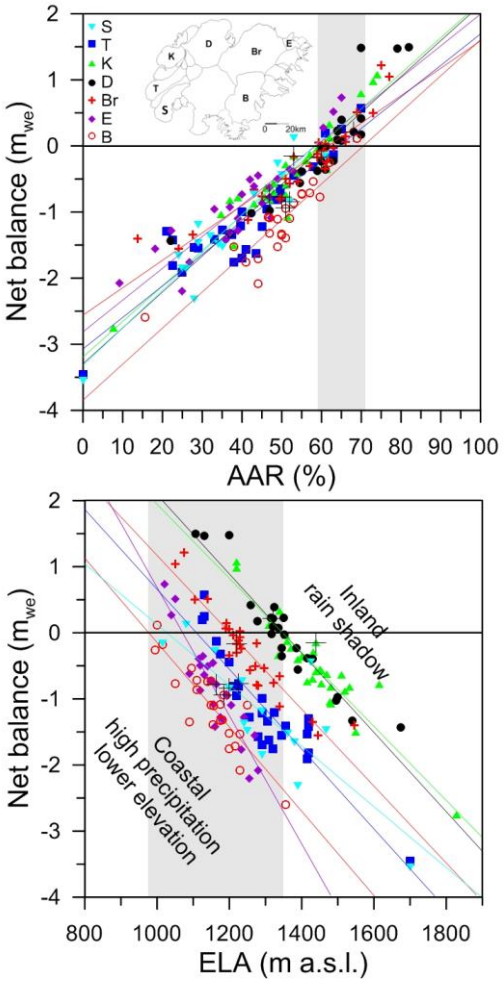

Figure 18. The relation between net annual balance (b_n) and accumulation area ratio (AAR) (upper) and b_n and equilibrium line altitude (ELA), for Vatnajökull outlets during the survey period. (This years points are marked with a black +).

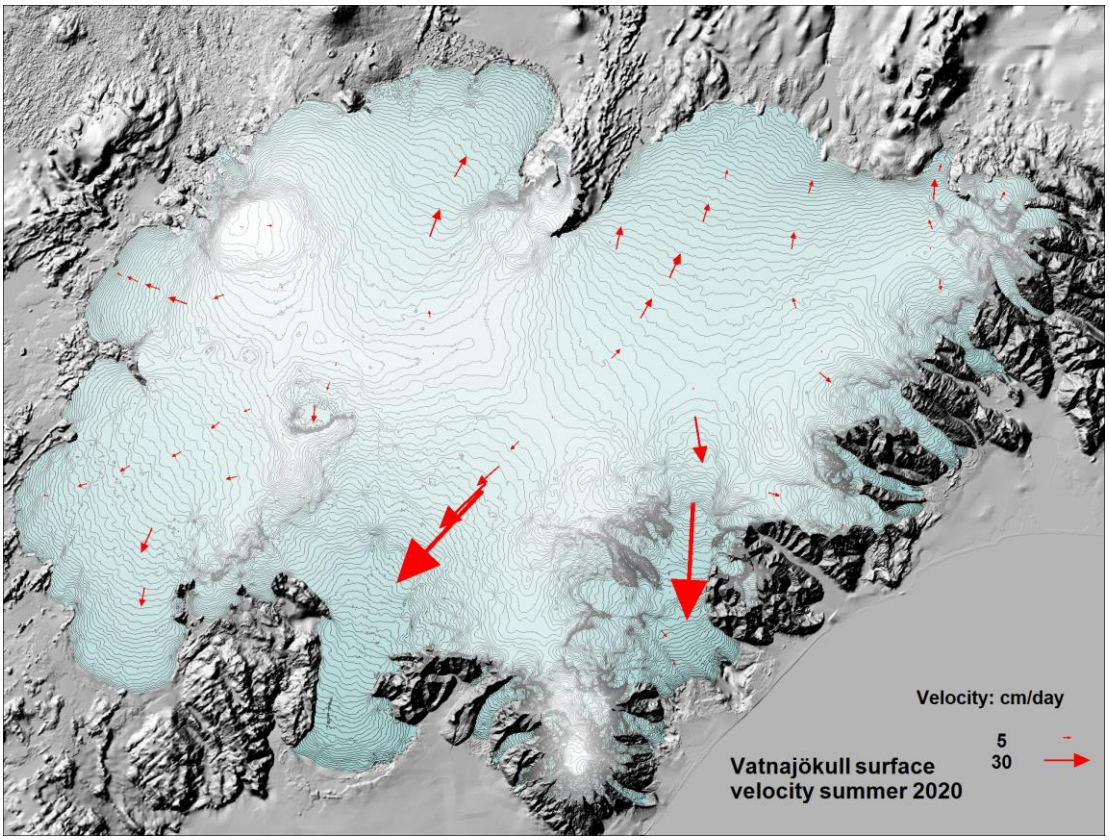

Figure 19. Average summer surface velocity at survey sites in 2019_20.

4. SURFACE VELOCITY MEASUREMENTS

The surface velocity of the glacier was calculated from DGPS (accuracy within 1 m), fast static (accuracy ~1 cm) and kinematic GPS (accuracy about ~10 cm) positioning of the ablation stakes. All sites were surveyed in spring and autumn (most kinematic, a few with DGPS), and many in June (kinematic) and in October (kinematic). At a few sites stakes from previous years were found and resurveyed, making it possible to calculate surface velocity over a year or longer time span. The average summer surface velocity is shown in Figure 19.

At sites close to the glacier terminus very small horizontal movement is measured. This indicates that the glacier snouts are almost stagnant. In the centre areas of some of the outlets especially close to the equilibrium line, there is an increase in velocity during summer compared to winter. The summer velocity is typically in the order of two-fold the winter velocity. This suggests that basal sliding is increased in the melting season, and is of the same magnitude as the deformation velocity.

To better understand the variable velocity continuous GPS has been run during summer at several sites.

From previous velocity measurements, surging of outlets has been predicted. Currently the increase in velocity at sites D05 and D07 (Fig. 20.) persists and suggests that Dyngjujökull may surge within a few years. The velocity at sites D07 and D05 is now similar to that in 1997 prior to the surge in 1998-2000 and the accumulation zone has thickened. To monitor velocity changes leading up to a surge GPS instrument were set up in spring to

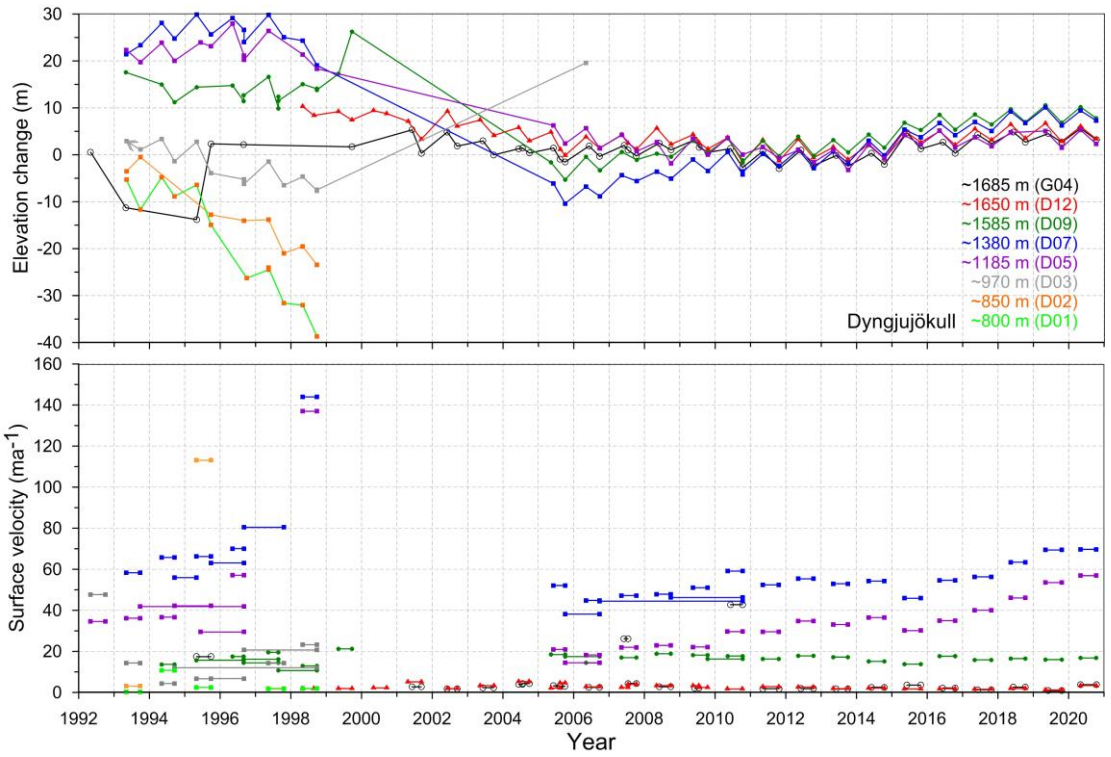

Figure 20. Surface elevation change relative to spring 2010 (upper panel) and average surface velocity (lower panel) at mb sites on Dyngjujökull in 1992 to 2020.

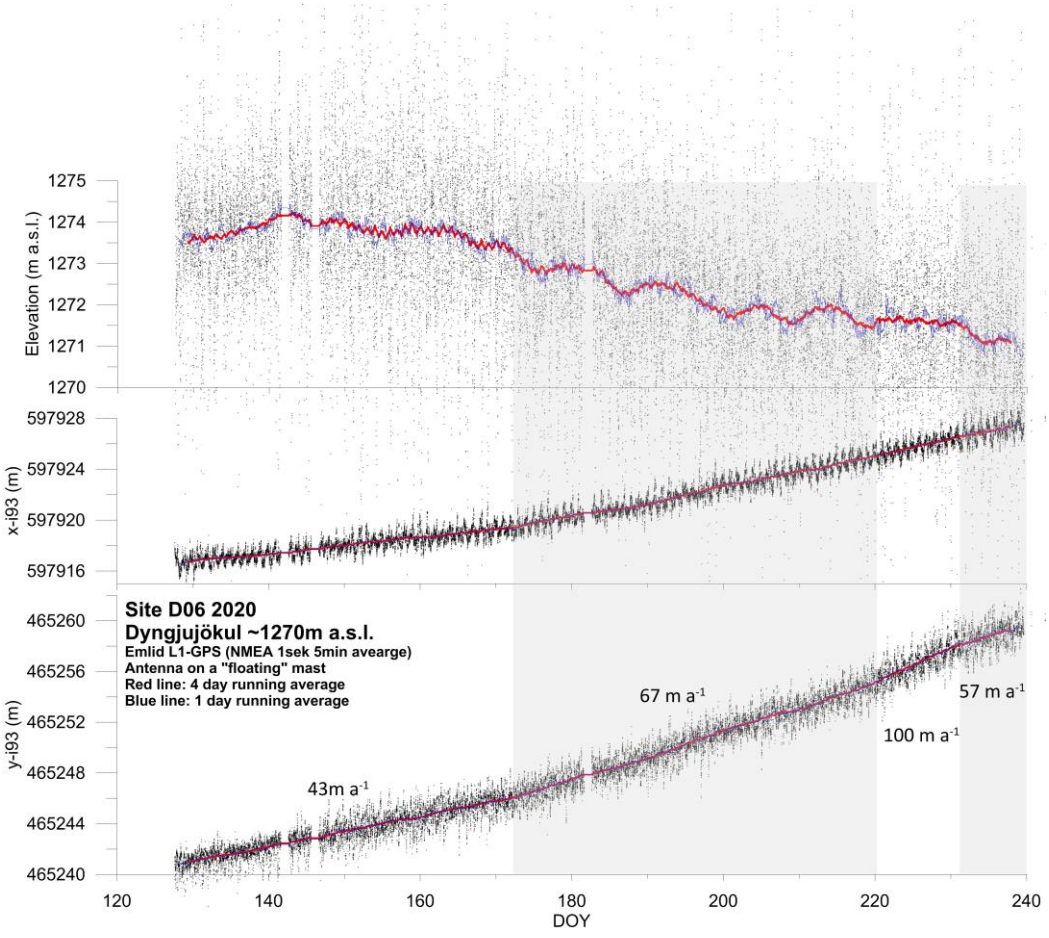

Figure 21. Surface elevation (top panel) and movement (easting in middle panel and northing in lowest panel) surveyed with continuous GPS survey at mb site D06 on Dyngjujökull in summer 2020.

continuously monitor movement at sites D05, D06 and D07. Unfortunately the instruments at quipped D05 and D07 were set to collect data at 5Hz, so their memory filled with only a month worth of data.
The data collected allows for post-processing to acquire more accuracy (~dm instead of ~m), but the processing has not been finished when this report is written. However the unprocessed data (Fig. 21) show mostly steady movement, increasing with start of the melt season in June and a further increase in August, probably related to lowering albedo. In September there is significant slowdown, nearing the spring velocity.
Most vehicles used in the survey are equipped with survey type GPS that collect data while driving. These are post-processed, to yield surface profiles with an accuracy of ~dm in horizontal and vertical. Location of all profiles in 2020 is shown in image 22.

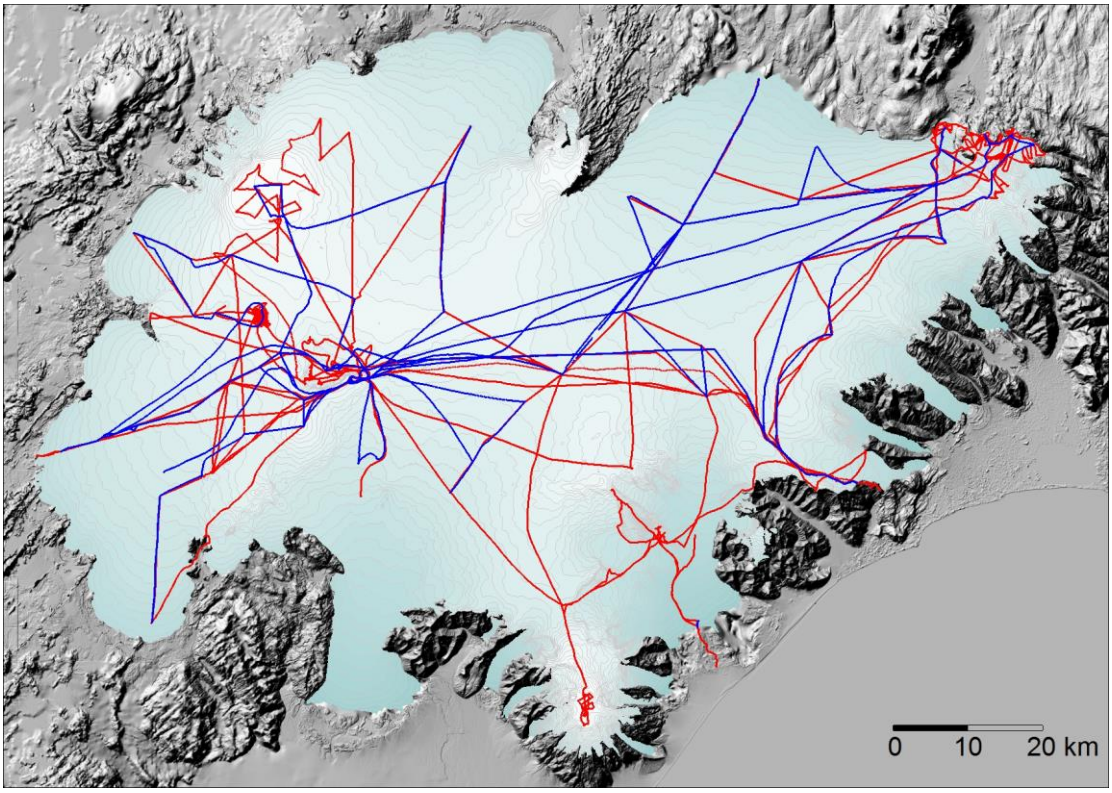

Figure 22. Location of surface elevation profiles surveyed in field trips on Vatnajökull in 2020. Survey in spring is shown with red and autumn survey in blue.

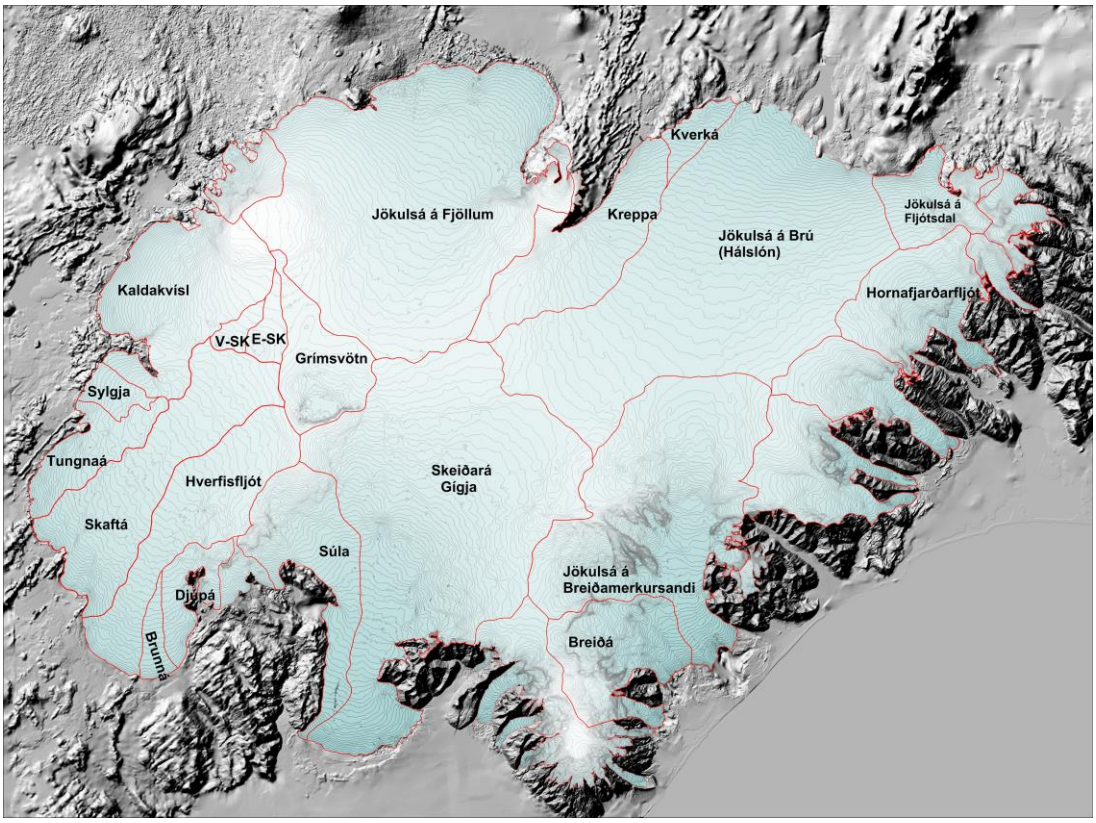

Figure 23. Water divides and drainage basins of selected rivers draining water from Vatnajökull, Súla is since summer 2016 diverted to Gígja.

5. Melt water runoff.

Water divides and drainage basins for rivers draining water from Vatnajökull have been defined from water pressure potential maps. The potential maps were produced from surface (year 2010) and bedrock DEMs.

Figure 23 shows the water divides and drainage areas for selected rivers draining melt water from Vatnajökull. The summer balance over the water basin is an estimate of meltwater contribution to rivers and groundwater storage. This estimate, however, does not include precipitation that falls as rain on the glacier, or snow that falls and melts during the summer. The meltwater contribution can be compared with river runoff at stream flow gauges closest to the glacier. For this comparison, we define the glaciological year from the start of October to the end of September and the period draining meltwater from the glacier during the summer from June through September. It would be misleading to include May in the summer period because runoff from the glacier melt in May is delayed due

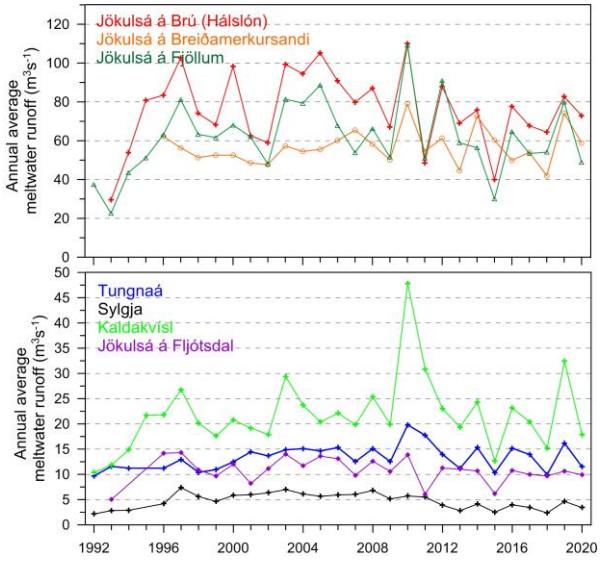

Figure 24. The temporal variation of average annual meltwater runoff to selected river catchments.

Table I. Melt water drainage to selected rivers in summer 2020.

Water Catchment:	Area (km^2)	ΣQ_s ($10^6 m^3$)	Q_s ($m^3 s^{-1}$)	Q_a ($m^3 s^{-1}$)	q_s ($ls^{-1}km^{-2}$)
Vatnajökull	7633,8	16036,0	1521,3	508,5	66,6
Tungnaá	109,9	362,9	34,4	11,5	104,7
Sylgja	38,7	107,7	10,2	3,4	88,2
Kaldakvísl	314,4	563,8	53,5	17,9	56,9
Jökulsá á Fjöllum	1088,5	1540,4	146,1	48,8	44,9
Kreppa	288,2	435,3	41,3	13,8	47,9
Kverka	36,8	160,5	15,2	5,1	138,3
Hálslón	1196,1	2299,2	218,1	72,9	61,0
Jökulsá á Fljótsdal	124,8	313,3	29,7	9,9	79,6
Jökulsá í Lóni	97,5	234,0	22,2	7,4	76,1
Hornafjarðarfljót	233,2	512,9	48,7	16,3	69,7
Jökulsá á Breiðamerkursandi	727,2	1854,4	175,9	58,8	80,9
Breiðá-Fjallsá	214,9	884,8	83,9	28,1	130,6
Skeiðará-Gígja	1393,5	2972,8	282,0	94,3	67,6
Brunná	31,8	151,1	14,3	4,8	150,7
Djúpá	74,0	235,0	22,3	7,5	100,7
Hverfisfljót	309,6	607,7	57,7	19,3	62,2
Skaftá	384,2	861,6	81,7	27,3	71,1
Grímsvötn	169,8	105,8	10,0	3,4	19,8
Eystri Skaftárketill	39,3	12,8	1,2	0,4	10,3
Vestari Skaftárketill	25,1	11,5	1,1	0,4	14,5
Hólmsá	160,8	381,5	36,2	12,1	75,2
Heinabergsvötn	223,9	585,8	55,6	18,6	83,0
Skjálfandafljót	95,7	107,3	10,2	3,4	35,6

ΣQ_s: total summer melt water; Q_s: average runoff (averaged over summer, 4 months, June – September)
Q_a: average runoff (averaged over a whole year); q_s : average runoff per km^2 (averaged over a whole year)

to refreezing during elimination of the cold wave and because of the contribution of the spring snow melt from the highlands to the runoff. Some melting also occurs during winter, especially in the terminus regions of the southern outlets.

Average melt water runoff to different rivers is given in Table I, and temporal variation of the average meltwater runoff in Fig. 24. The average specific runoff (q_s) differs from basin to basin from ~10 to ~140 $ls^{-1}km^{-2}$. This is mainly due to different elevation distributions, for example, the water drainage basins for Tungnaá and Kverká are within the ablation area, while that of Grímsvötn and Skaftárkatlar are high in the accumulation zone.

6. Conclusions

In the glaciological year 2019_20 the winter balance for Vatnajökull exceeded the average, over the observation period from 1991_92, by ~8%.
The total summer mass loss was 7% less than average since 1995 (but at average since 191_92).
The net balance was negative as it has been since 1994_95 (except 2014_15), but mass loss only 50% of the average since 1994_95 (70% of the average since 1991_92).
In the past few years, the about 20 year period of high mass loss seemed to have halted; but last year the mass loss was high again, but now less so.
The total mass loss over the 28 year survey period is 12.4 m_{we} (ice volume of ~111 km^3) since 1991_92 (or since 1994_95, 15,9 m_{we}, ice volume of ~139 km^3)). The volume loss since 1991_92 amounts to ~3.7% of total ice volume (~4.6% since 1994_95).
In addition to surface melt, mass is lost due to calving, geothermal melting at the glacier bed and melt from frictional energy due to ice deformation and sliding. This is estimated to be close to 0.2 $m_{we}a^{-1}$ for Vatnajökull
(Tómas Jóhannesson, Bolli Pálmason, Árni Hjartarson, Jarosch, A., Eyjólfur Magnússon, Belart, J., og Magnús Tumi Guðmundsson. (2020). Non-surface mass balance of glaciers in Iceland. J. of Glaciology. 66, 685–697. doi:10.1017/jog.2020.37).

Glacier surface meltwater runoff in summer 2020 (estimated from summer surface balance only, summer rain and snow that falls and melts during summer, calving and geothermal and internal melting, is not included; averages refer to the survey period of each outlet): to Tungnaá 86% of the average, 82 % of the average to Kaldakvísl, 79 % of the average to Jökulsá á Fjöllum, 96% of the average to Hálslón, close to average to Jökulsá í Fljótsdal and 3% over the average to Jökulsá á Breiðamerkursandi.
Surface velocity measurements suggest that Dyngjujökull is in the first phase of a surge, and will likely complete a surge cycle within the next few years.

Surface mass balance summary 2019_20:

B_w = 13.57 km^3_{we}
B_s = -15.94 km^3_{we}
B_n = -2.37 km^3_{we}
AAR = 59%

Specific Values:

b_w = 1.75 m_{we}
b_s = -2.05 m_{we}
b_n = -0.30 m_{we}

Appendix A: Surface mass balance at measurement sites 2019_20.

b_w: specific winter balance, **b_s**: specific summer balance, **b_n**: specific net balance, **l_a**: new snow in autumn (all in water equivalent).

Site	Position				Elevation	Date	Date	b_w	b_s	b_n	la
	Latitude		Longitude		(m a.s.l.)	in spring	in autumn	(m)	(m)	(m)	(m)
B09-20	64	44,8344	16	5,8532	720,2	20200430	20201009	0,07	-5,902	-5,832	0,04
B10-20	64	43,6871	16	6,6980	774,4	20200430	20201009	0,10	-4,627	-4,527	0,04
B11-20	64	40,9360	16	10,4688	951,1	20200430	20201009	1,02	-3,783	-2,763	0,07
B12-20	64	38,2673	16	14,1395	1078,5	20200430	20201009	1,31	-2,732	-1,422	0,11
B13-20	64	34,5777	16	19,6424	1220,9	20200501	20201009	1,59	-1,600	-0,010	0,16
B14-20	64	31,6407	16	24,7020	1320,6	20200430	20201009	1,76	-1,070	0,690	0,18
B15-20	64	28,4924	16	30,0268	1403,6	20200430	20201009	2,19	-0,942	1,248	0,19
B16-20	64	24,1269	16	40,8871	1530,3	20200501	20201009	2,44	-0,988	1,452	0,35
B17-20	64	36,7316	16	28,7950	1218,5	20200430	20201009	1,51	-1,969	-0,459	0,09
Br1-20	64	5,9626	16	19,8204	114,9	20200501	20201010	-0,47	-9,010	-9,483	0
Br2-19	64	6,3640	16	22,5339	192,1	20200501	20201010	0,25	-8,230	-7,980	0
Br3-19	64	8,4427	16	24,0155	370,1	20200501	20201010	0,83	-5,730	-4,905	0
Br5-20	64	13,5316	16	19,2052	674,7	20200505	20200000	0,80			0
Br7-20	64	22,1367	16	16,9221	1247,1	20200505	20201009	2,52	-2,064	0,456	0,25
B07-20	64	25,7966	16	17,4682	1358,8	20200604	20201009	2,13	-1,236	0,894	0,23
BB0-20	64	22,7094	16	5,0534	1519,8	20200429	20201008	2,48	-0,794	1,686	0,35
Bru-20	64	39,7487	15	56,5467	898,2	20200430	20201008	0,96	-4,191	-3,231	0,02
Bud-20	64	35,9956	15	59,8863	1143,7	20200430	20201008	1,67	-2,444	-0,774	0,12
B18-20	64	31,5604	16	0,1255	1317,0	20200429	20201008	2,17	-1,432	0,738	0,3
B19-20	64	27,9947	15	55,9898	1440,4	20200429	20201008	2,73	-0,402	2,328	0,4
D05-20	64	42,2242	16	54,6860	1205,5	20200502	20201010	1,25	-2,132	-0,882	0,05
D07-20	64	38,2837	16	59,2504	1377,8	20200502	20201010	1,60	-1,137	0,462	0,21
D09-20	64	31,7859	17	0,5942	1587,7	20200502	20201010	1,86	-0,554	1,302	0,26
D12-20	64	28,9722	17	0,1782	1650,6	20200502	20201010	2,20	-0,217	1,986	0,33
E01-20	64	40,6362	15	34,8451	762,5	20200429	20201008	0,55	-6,058	-5,508	0,04
E02-20	64	39,1225	15	35,9877	952,5	20200429	20201008	0,87	-4,659	-3,789	0,05
E03-20	64	36,6583	15	36,8996	1190,3	20200429	20201008	1,81	-1,412	0,400	0,35
E04-20	64	34,9514	15	37,1458	1290,2	20200429	20201008	2,44	-1,354	1,086	0,35
K01-20	64	35,1667	17	51,8313	1047,8	20200503	20201012	1,18	-4,132	-2,952	0,02
K02-20	64	34,8091	17	49,6875	1171,4	20200503	20201012	1,05	-3,048	-1,998	0,07
K03-20	64	34,2381	17	46,3986	1294,5	20200503	20201012	0,96	-2,221	-1,260	0,19
K04-20	64	33,2119	17	42,2525	1487,7	20200503	20201012	1,48	-1,073	0,402	0,18
K05-20	64	33,4462	17	35,4567	1680,5	20200503	20201012	1,76	-0,456	1,302	0,28
K06-20	64	38,3556	17	31,3207	1946,8	20200503	20201010	2,16	0,420	2,580	0,41
K07-20	64	29,1062	17	42,0344	1533,4	20200503	20201012	1,58	-0,854	0,726	0,28
S01-20	64	7,0150	17	49,9749	715,1	20200503	20201010	0,60	-5,416	-4,815	0
S02-20	64	12,1596	17	48,9824	1003	20200503	20201010	2,12	-2,844	-0,720	0,08
S04-20	64	16,1768	17	48,1899	1158	20200503	20201010	1,77	-1,932	-0,162	0,14
S05-20	64	20,5123	17	34,0025	1452	20200503	20201010	1,91	-0,890	1,020	0,32
Haab-20	64	20,9569	17	24,1197	1732	20200503	20201010	1,97	-0,030	1,940	0,56

T02-21	64	19,4751	18	4,5708	892,3	20200504	20201012	0,97	-4,327	-3,357	0
T03-20	64	20,2038	17	58,5835	1068	20200504	20201012	0,83	-3,476	-2,646	0,09
T04-20	64	21,3313	17	51,5132	1222,2	20200504	20201012	1,70	-1,727	-0,027	0,13
T05-20	64	22,2696	17	42,9877	1346,7	20200504	20201012	1,78	-1,222	0,558	0,22
T06-20	64	24,2681	17	36,5171	1469,4	20200504	20201012	1,92	-0,762	1,158	0,25
T07-20	64	25,2960	17	31,2045	1564,9	20200504	20201012	1,95	-0,552	1,398	0,3
T08-20	64	26,2939	17	27,7547	1637,8	20200503	20201010	1,88	-0,320	1,560	0,29
Bor-20	64	24,9372	17	20,1473	1441,8	20200503	20201012	2,05	-1,534	0,516	0,35
Borth-20	64	25,0253	17	19,1862	1447,0	20200502	20201012	2,34	-1,512	0,828	0,4
G02-20	64	26,8585	17	17,7141	1568,2	20200502	20201012	1,80	-0,582	1,218	0,26
G03-20	64	28,4364	17	16,3288	1660,9	20200502	20201012	1,83	-0,354	1,476	0,35
G04-20	64	30,0229	17	15,0295	1689,9	20200502	20201012	1,97	-0,392	1,578	0,33
Go1-20	64	33,9706	17	24,9438	1761,6	20200503	20201010	1,99	-0,298	1,692	0,29
Barc-20	64	38,4148	17	26,7664	1899,0	20200503	20201010	2,38	0,122	2,502	0,25
Skf00-20	64	15,4750	15	54,0832	949,1	20200428	20201008	2,13	-2,589	-0,459	0
Hof01-20	64	32,3361	15	35,8359	1143,4	20200429	20201008	1,74	-1,650	0,090	0,12
Skf01-20	64	18,0083	16	4,9996	1284,8	20200428	20201008	2,86	-1,300	1,560	0,25
Fl01-20	64	26,1558	15	55,6279	1348,8	20200429	20201008	2,81	-1,010	1,800	0,25
Ske02-20	64	15,9093	17	0,0517	1182,5	20200501	20201010	1,75	-1,654	0,096	0,14
Ske03-20	64	18,0586	16	56,1563	1301,8	20200501	20201010	2,44	-1,204	1,236	0,23
Ske04-20	64	20,1356	16	51,8170	1401,2	20200501	20201010	2,08	-1,004	1,080	0,23
Ske05-20	64	22,2321	16	47,2351	1475,7	20200501	20201010	2,25	-0,924	1,326	0,32
Oer01-20	63	59,8757	16	38,9931	1828,0	20200502	20200901	4,74	2,070	6,810	0
E10-20	64	39,1495	15	30,0094	1293,2	20200429	20201000	3,81			0
E08-20	64	39,7158	15	23,8484	955	20200429	20201013	1,21	-3,475	-2,268	0,04
E09-20	64	39,9893	15	28,2674	981	20200429	20201013	1,730	-3,431	-1,701	0,053
E07-20	64	38,4052	15	24,6752	1074	20200429	20201013	1,860	-2,724	-0,864	0,053

Appendix B: Surface mass balance distribution by elevation in 2019_20.

ΔS : area in elevation range, $\sum\Delta S$: cumulative area above given elevation, b_w: specific winter balance, b_s: specific summer balance. b_n: specific winter balance, ΔB_w : winter balance at a given elevation range, $\sum\Delta B_w$: cumulative winter balance above given elevation, ΔB_s summer balance at a given elevation range, $\sum\Delta B_s$: cumulative summer balance above given elevation, ΔB_n: net annual balance in a given elevation range, $\sum B_n$: cumulative net annual balance above given elevation.

Vatnajökull

Elevation (m a.s.l.)			ΔS (km^2)	$\sum\Delta S$ (km^2)	b_w (mm)	b_s (mm)	b_n (mm)	ΔB_w ($10^6 m^3$)	$\sum\Delta B_w$ ($10^6 m^3$)	ΔB_s ($10^6 m^3$)	$\sum\Delta B_s$ ($10^6 m^3$)	ΔB_n ($10^6 m^3$)	$\sum B_n$ ($10^6 m^3$)
2000	2050	2025	0,4	0,4	5109	2756	7866	1,8	1,8	1,0	1,0	2,8	2,8
1950	2000	1975	7,1	7,5	2806	960	3766	19,8	21,7	6,8	7,8	26,6	29,4
1900	1950	1925	41,5	49,0	2401	471	2872	99,6	121,3	19,6	27,3	119,2	148,6
1850	1900	1875	44	93,0	2577	408	2985	113,3	234,6	18,0	45,3	131,3	279,9
1800	1850	1825	45,6	138,6	2775	466	3241	126,6	361,2	21,3	66,6	147,9	427,8
1750	1800	1775	54,6	193,2	2463	115	2579	134,5	495,7	6,3	72,9	140,8	568,6
1700	1750	1725	114	306,8	2174	-197	1977	247,0	742,7	-22,4	50,4	224,5	793,1
1650	1700	1675	217	523,5	2086	-313	1773	452,1	1194,8	-67,9	-17,5	384,2	1177,4
1600	1650	1625	372	895,2	2136	-399	1737	794,1	1988,9	-148,4	-165,9	645,7	1823,0
1550	1600	1575	358	1253,3	2135	-590	1544	764,7	2753,6	-211,5	-377,3	553,2	2376,3
1500	1550	1525	423	1676,1	2121	-776	1345	897,1	3650,7	-328,3	-705,6	568,8	2945,1
1450	1500	1475	454	2130,2	2115	-883	1232	960,8	4611,5	-401,2	-1106,8	559,6	3504,7
1400	1450	1425	506	2636,2	2163	-959	1204	1094,8	5706,3	-485,4	-1592,2	609,4	4114,1
1350	1400	1375	547	3183,0	2125	-1105	1020	1162,3	6868,6	-604,3	-2196,5	558,0	4672,1
1300	1350	1325	539	3722,2	2051	-1290	761	1106,2	7974,8	-695,5	-2892,0	410,7	5082,8
1250	1300	1275	506	4228,2	1968	-1508	459	995,8	8970,6	-763,2	-3655,2	232,6	5315,4
1200	1250	1225	447	4675,5	1829	-1746	83	818,3	9788,9	-781,0	-4436,3	37,3	5352,7
1150	1200	1175	397	5072,0	1711	-2050	-339	678,5	10467,5	-813,2	-5249,4	-134,6	5218,0
1100	1150	1125	353	5424,8	1620	-2365	-744	571,9	11039,3	-834,6	-6084,0	-262,7	4955,3
1050	1100	1075	311	5735,3	1539	-2705	-1165	478,1	11517,4	-839,9	-6923,9	-361,8	4593,6
1000	1050	1025	290	6025,2	1464	-3047	-1583	424,5	11941,9	-883,6	-7807,5	-459,1	4134,5
950	1000	975	259	6284,6	1373	-3356	-1983	356,2	12298,1	-870,7	-8678,2	-514,5	3619,9
900	950	925	224	6509,0	1280	-3606	-2325	287,4	12585,5	-809,4	-9487,6	-522,0	3098,0
850	900	875	195	6704,3	1167	-3850	-2683	228,0	12813,6	-752,1	-10239,6	-524,1	2573,9
800	850	825	179	6883,4	1039	-4120	-3081	186,2	12999,8	-738,2	-10977,9	-552,0	2021,9
750	800	775	158	7041,6	904	-4434	-3529	143,2	13142,9	-701,5	-11679,3	-558,3	1463,6
700	750	725	129	7170,4	803	-4744	-3940	103,4	13246,4	-611,0	-12290,3	-507,5	956,0
650	700	675	109	7278,9	786	-4909	-4122	85,4	13331,7	-532,7	-12823,0	-447,3	508,7
600	650	625	66,6	7345,5	821	-4913	-4091	54,8	13386,5	-327,3	-13150,4	-272,6	236,1
550	600	575	61,5	7407,0	823	-5007	-4184	50,6	13437,1	-307,9	-13458,2	-257,2	-21,1
500	550	525	49,6	7456,6	765	-5217	-4451	38,0	13475,1	-258,8	-13717,0	-220,8	-241,9
450	500	475	37,1	7493,7	726	-5447	-4721	27,0	13502,1	-202,3	-13919,4	-175,4	-417,3
400	450	425	41,1	7534,8	690	-5703	-5013	28,4	13530,5	-234,3	-14153,7	-205,9	-623,2
350	400	375	38,5	7573,3	591	-5992	-5401	22,8	13553,3	-230,9	-14384,6	-208,1	-831,3
300	350	325	34,5	7607,8	481	-6384	-5902	16,6	13569,9	-220,5	-14605,1	-203,8	-1035,1
250	300	275	32,9	7640,7	365	-6934	-6569	12,0	13581,9	-227,9	-14833,0	-215,9	-1251,1
200	250	225	31,1	7671,8	228	-7587	-7358	7,1	13589,0	-236,1	-15069,1	-229,0	-1480,1
150	200	175	31	7702,8	53	-8202	-8149	1,6	13590,7	-254,1	-15323,2	-252,5	-1732,6
100	150	125	27,3	7730,1	-146	-8734	-8880	-4,0	13586,7	-238,6	-15561,9	-242,6	-1975,2
50	100	75	20,5	7750,6	-293	-9237	-9530	-6,0	13580,7	-189,5	-15751,3	-195,5	-2170,7
0	50	25	19,9	7770,5	-376	-9668	-10044	-7,5	13573,2	-192,0	-15943,3	-199,5	-2370,2

Tungnaárjökull

Elevation (m a.s.l.)			ΔS (km^2)	∑ΔS (km^2)	b_w (mm)	b_s (mm)	b_n (mm)	ΔB_w ($10^6 m^3$)	$\sum\Delta B_w$ ($10^6 m^3$)	ΔB_s ($10^6 m^3$)	$\sum\Delta B_s$ ($10^6 m^3$)	ΔB_n ($10^6 m^3$)	$\sum B_n$ ($10^6 m^3$)
1650	1700	1675	1,7	1,7	1884	-346	1538	3,1	3,1	-0,6	-0,6	2,6	2,6
1600	1650	1625	12,2	13,9	1888	-372	1516	23,0	26,1	-4,5	-5,1	18,5	21,0
1550	1600	1575	16,4	30,3	1892	-487	1405	31,0	57,1	-8,0	-13,1	23,0	44,0
1500	1550	1525	15,9	46,2	1881	-619	1261	29,9	87,0	-9,9	-22,9	20,1	64,1
1450	1500	1475	18,4	64,6	1854	-747	1107	34,1	121,1	-13,7	-36,7	20,4	84,4
1400	1450	1425	23,2	87,8	1840	-928	912	42,6	163,7	-21,5	-58,2	21,1	105,5
1350	1400	1375	21,2	109,0	1804	-1132	672	38,3	202,0	-24,0	-82,2	14,2	119,8
1300	1350	1325	27,2	136,2	1745	-1330	415	47,4	249,4	-36,2	-118,4	11,3	131,1
1250	1300	1275	20,7	156,9	1718	-1513	205	35,5	284,9	-31,3	-149,6	4,2	135,3
1200	1250	1225	22,6	179,5	1670	-1775	-104	37,7	322,6	-40,0	-189,7	-2,4	133,0
1150	1200	1175	20,8	200,3	1596	-2283	-687	33,3	355,9	-47,6	-237,3	-14,3	118,6
1100	1150	1125	18	218,3	1485	-2888	-1402	26,7	382,6	-51,9	-289,1	-25,2	93,4
1050	1100	1075	17,3	235,6	1398	-3368	-1969	24,2	406,8	-58,2	-347,4	-34,0	59,4
1000	1050	1025	16,7	252,3	1318	-3698	-2379	22,1	428,8	-61,8	-409,2	-39,8	19,6
950	1000	975	16,1	268,4	1212	-3938	-2726	19,5	448,4	-63,5	-472,7	-44,0	-24,3
900	950	925	16,3	284,7	1104	-4167	-3062	18,0	466,4	-68,1	-540,7	-50,0	-74,3
850	900	875	12,5	297,2	998	-4413	-3414	12,5	478,9	-55,1	-595,8	-42,6	-117,0
800	850	825	12,9	310,1	906	-4680	-3773	11,7	490,6	-60,6	-656,4	-48,8	-165,8
750	800	775	10,5	320,6	788	-5021	-4232	8,2	498,8	-52,5	-708,9	-44,3	-210,1
700	750	725	7,2	327,8	697	-5364	-4666	5,0	503,9	-38,6	-747,5	-33,6	-243,6
650	700	675	2,4	330,2	635	-5592	-4957	1,5	505,4	-13,4	-760,8	-11,8	-255,5

Sylgjujökull

Elevation (m a.s.l.)			ΔS (km^2)	∑ΔS (km^2)	b_w (mm)	b_s (mm)	b_n (mm)	ΔB_w ($10^6 m^3$)	$\sum\Delta B_w$ ($10^6 m^3$)	ΔB_s ($10^6 m^3$)	$\sum\Delta B_s$ ($10^6 m^3$)	ΔB_n ($10^6 m^3$)	$\sum B_n$ ($10^6 m^3$)
1600	1650	1625	1,4	1,4	1849	-464	1384	2,5	2,5	-0,6	-0,6	1,9	1,9
1550	1600	1575	5	6,4	1818	-538	1280	9,1	11,6	-2,7	-3,3	6,4	8,3
1500	1550	1525	18,7	25,1	1691	-735	955	31,6	43,3	-13,7	-17,1	17,9	26,2
1450	1500	1475	13,7	38,8	1644	-910	733	22,5	65,8	-12,5	-29,6	10,0	36,2
1400	1450	1425	8,2	47,0	1648	-1020	627	13,6	79,3	-8,4	-38,0	5,2	41,4
1350	1400	1375	5,6	52,6	1635	-1140	495	9,2	88,5	-6,4	-44,4	2,8	44,2
1300	1350	1325	5,2	57,8	1585	-1314	270	8,2	96,7	-6,8	-51,2	1,4	45,6
1250	1300	1275	9,8	67,6	1523	-1511	11	14,9	111,6	-14,7	-65,9	0,1	45,7
1200	1250	1225	11,6	79,2	1462	-1827	-365	17,0	128,6	-21,3	-87,2	-4,3	41,4
1150	1200	1175	13,1	92,3	1387	-2270	-882	18,2	146,8	-29,7	-116,9	-11,6	29,8
1100	1150	1125	12,3	104,6	1300	-2805	-1504	16,0	162,7	-34,4	-151,3	-18,5	11,4
1050	1100	1075	11,4	116,0	1207	-3314	-2106	13,8	176,5	-37,8	-189,1	-24,0	-12,6
1000	1050	1025	11,2	127,2	1112	-3942	-2830	12,5	188,9	-44,2	-233,3	-31,7	-44,3
950	1000	975	3,6	130,8	1021	-4452	-3430	3,7	192,6	-15,9	-249,2	-12,3	-56,6
900	950	925	1,5	132,3	959	-4794	-3835	1,5	194,1	-7,3	-256,5	-5,9	-62,5
850	900	875	0	132,3	875	-5044	-4168	0,0	194,1	-0,2	-256,7	-0,2	-62,6

Köldukvíslarjökul

Elevation (m a.s.l.)			ΔS (km^2)	∑ΔS (km^2)	b_w (mm)	b_s (mm)	b_n (mm)	ΔB_w ($10^6 m^3$)	$\sum\Delta B_w$ ($10^6 m^3$)	ΔB_s ($10^6 m^3$)	$\sum\Delta B_s$ ($10^6 m^3$)	ΔB_n ($10^6 m^3$)	$\sum B_n$ ($10^6 m^3$)
1950	2000	1975	0,7	0,7	2150	484	2634	1,4	1,4	0,3	0,3	1,7	1,7
1900	1950	1925	13,8	14,5	2204	356	2561	30,5	31,9	4,9	5,3	35,4	37,2
1850	1900	1875	6,5	21,0	2160	189	2349	14,1	46,0	1,2	6,5	15,3	52,5
1800	1850	1825	6,1	27,1	2111	48	2159	12,9	58,9	0,3	6,8	13,2	65,6
1750	1800	1775	10,1	37,2	2077	-43	2033	20,9	79,7	-0,4	6,3	20,4	86,1
1700	1750	1725	17,2	54,4	1945	-248	1696	33,5	113,2	-4,3	2,1	29,2	115,3
1650	1700	1675	16	70,4	1778	-465	1313	28,4	141,7	-7,4	-5,4	21,0	136,3
1600	1650	1625	14,2	84,6	1683	-626	1057	23,9	165,6	-8,9	-14,3	15,0	151,3
1550	1600	1575	18,6	103,2	1612	-778	834	30,0	195,6	-14,5	-28,8	15,5	166,8
1500	1550	1525	20	123,2	1540	-939	600	30,7	226,3	-18,8	-47,5	12,0	178,8
1450	1500	1475	19,3	142,5	1481	-1120	360	28,6	254,9	-21,6	-69,1	7,0	185,8
1400	1450	1425	15	157,5	1421	-1316	105	21,2	276,2	-19,7	-88,8	1,6	187,3
1350	1400	1375	14,8	172,3	1343	-1592	-248	19,9	296,1	-23,6	-112,4	-3,7	183,7
1300	1350	1325	17,1	189,4	1260	-1931	-670	21,6	317,7	-33,1	-145,5	-11,5	172,2
1250	1300	1275	17,9	207,3	1173	-2271	-1097	21,0	338,7	-40,7	-186,2	-19,7	152,5
1200	1250	1225	16,9	224,2	1096	-2636	-1540	18,5	357,2	-44,5	-230,7	-26,0	126,5
1150	1200	1175	16,2	240,4	1062	-3049	-1987	17,2	374,4	-49,3	-280,0	-32,1	94,4
1100	1150	1125	14,3	254,7	1091	-3520	-2428	15,6	390,0	-50,3	-330,3	-34,7	59,6
1050	1100	1075	12,9	267,6	1131	-3895	-2763	14,6	404,5	-50,1	-380,4	-35,5	24,1
1000	1050	1025	10,3	277,9	1134	-4138	-3004	11,7	416,2	-42,7	-423,1	-31,0	-6,9
950	1000	975	8,8	286,7	1103	-4295	-3192	9,7	426,0	-37,9	-461,0	-28,2	-35,1
900	950	925	2,6	289,3	1080	-4428	-3348	2,8	428,8	-11,5	-472,5	-8,7	-43,8

Dyngjujökull

Elevation (m a.s.l.)			ΔS (km^2)	∑ΔS (km^2)	b_w (mm)	b_s (mm)	b_n (mm)	ΔB_w ($10^6 m^3$)	$\sum\Delta B_w$ ($10^6 m^3$)	ΔB_s ($10^6 m^3$)	$\sum\Delta B_s$ ($10^6 m^3$)	ΔB_n ($10^6 m^3$)	$\sum B_n$ ($10^6 m^3$)
1950	2000	1975	2,4	2,4	2135	444	2579	5,1	5,1	1,1	1,1	6,1	6,1
1900	1950	1925	17,7	20,1	2260	304	2564	40,1	45,2	5,4	6,5	45,5	51,6
1850	1900	1875	21,7	41,8	2267	84	2352	49,1	94,3	1,8	8,3	51,0	102,6
1800	1850	1825	13,2	55,0	2183	-93	2090	28,8	123,1	-1,2	7,1	27,5	130,1
1750	1800	1775	15,5	70,5	2136	-201	1935	33,0	156,1	-3,1	4,0	29,9	160,0
1700	1750	1725	32,4	102,9	2105	-285	1819	68,3	224,4	-9,3	-5,3	59,0	219,1
1650	1700	1675	73,9	176,8	2079	-328	1751	153,7	378,1	-24,3	-29,6	129,5	348,5
1600	1650	1625	120	297,1	2013	-390	1622	242,1	620,2	-47,0	-76,6	195,1	543,6
1550	1600	1575	96,1	393,2	1906	-551	1355	183,2	803,4	-52,9	-129,5	130,2	673,9
1500	1550	1525	87,5	480,7	1841	-650	1190	161,1	964,5	-56,9	-186,5	104,2	778,0
1450	1500	1475	73	553,7	1760	-775	984	128,6	1093,1	-56,7	-243,2	71,9	850,0
1400	1450	1425	60,5	614,2	1687	-924	762	102,1	1195,2	-55,9	-299,1	46,1	896,1
1350	1400	1375	48,1	662,3	1614	-1107	506	77,6	1272,8	-53,2	-352,3	24,4	920,5
1300	1350	1325	36,5	698,8	1538	-1305	232	56,2	1328,9	-47,7	-400,0	8,5	929,0
1250	1300	1275	39,6	738,4	1444	-1528	-84	57,2	1386,1	-60,5	-460,5	-3,3	925,6
1200	1250	1225	44	782,4	1322	-1819	-496	58,2	1444,4	-80,1	-540,6	-21,9	903,8
1150	1200	1175	44,4	826,8	1196	-2239	-1043	53,1	1497,5	-99,5	-640,1	-46,3	857,4
1100	1150	1125	42,3	869,1	1099	-2654	-1555	46,4	1543,9	-112,2	-752,3	-65,7	791,7
1050	1100	1075	30,6	899,7	1035	-3107	-2071	31,7	1575,6	-95,1	-847,4	-63,4	728,3
1000	1050	1025	30,9	930,6	964	-3493	-2529	29,8	1605,4	-107,9	-955,2	-78,1	650,1
950	1000	975	28,8	959,4	848	-3897	-3048	24,4	1629,8	-112,2	-1067,5	-87,8	562,4
900	950	925	24,2	983,6	706	-4278	-3572	17,1	1646,9	-103,6	-1171,0	-86,5	475,9
850	900	875	21	1004,6	582	-4642	-4059	12,2	1659,2	-97,6	-1268,7	-85,4	390,5
800	850	825	18,7	1023,3	486	-5004	-4518	9,1	1668,3	-93,6	-1362,2	-84,5	306,0
750	800	775	12,3	1035,6	408	-5395	-4987	5,0	1673,3	-66,3	-1428,5	-61,2	244,8
700	750	725	3,7	1039,3	348	-5848	-5500	1,3	1674,6	-21,5	-1450,0	-20,2	224,6

Brúarjökull

Elevation (m a.s.l.)			ΔS (km^2)	∑ΔS (km^2)	b_w (mm)	b_s (mm)	b_n (mm)	ΔB_w ($10^6 m^3$)	$\sum\Delta B_w$ ($10^6 m^3$)	ΔB_s ($10^6 m^3$)	$\sum\Delta B_s$ ($10^6 m^3$)	ΔB_n ($10^6 m^3$)	$\sum B_n$ ($10^6 m^3$)
1900	1950	1925	0	0,0	1901	-238	1662	0,0	0,0	0,0	0,0	0,0	0,0
1850	1900	1875	1,2	1,2	2029	-177	1851	2,4	2,5	-0,2	-0,2	2,2	2,3
1800	1850	1825	4,4	5,6	2165	-91	2073	9,6	12,0	-0,4	-0,6	9,2	11,4
1750	1800	1775	2,8	8,4	2298	-163	2135	6,6	18,6	-0,5	-1,1	6,1	17,5
1700	1750	1725	3,9	12,3	2373	-212	2160	9,2	27,8	-0,8	-1,9	8,4	25,9
1650	1700	1675	5,5	17,8	2372	-284	2088	13,0	40,8	-1,6	-3,5	11,4	37,4
1600	1650	1625	51	68,8	2300	-391	1908	117,4	158,2	-20,0	-23,5	97,4	134,8
1550	1600	1575	47,4	116,2	2383	-640	1742	112,9	271,1	-30,3	-53,8	82,5	217,3
1500	1550	1525	73,6	189,8	2375	-845	1530	174,9	446,0	-62,2	-116,0	112,7	330,0
1450	1500	1475	80,3	270,1	2317	-926	1391	186,0	632,0	-74,4	-190,4	111,7	441,7
1400	1450	1425	114	384,0	2326	-915	1411	264,9	897,0	-104,2	-294,6	160,7	602,4
1350	1400	1375	159	542,6	2184	-1048	1136	346,5	1243,5	-166,3	-460,9	180,2	782,6
1300	1350	1325	148	691,0	2011	-1172	839	298,5	1542,0	-174,0	-634,8	124,6	907,2
1250	1300	1275	139	830,1	1904	-1419	485	264,9	1806,9	-197,4	-832,2	67,5	974,7
1200	1250	1225	117	947,4	1767	-1724	43	207,3	2014,2	-202,2	-1034,5	5,1	979,8
1150	1200	1175	100	1047,4	1634	-2082	-448	163,4	2177,7	-208,3	-1242,8	-44,9	934,9
1100	1150	1125	80,4	1127,8	1494	-2473	-979	120,3	2297,9	-199,0	-1441,8	-78,8	856,1
1050	1100	1075	65,6	1193,4	1363	-2840	-1476	89,5	2387,4	-186,3	-1628,1	-96,9	759,3
1000	1050	1025	57,9	1251,3	1236	-3235	-1998	71,6	2459,0	-187,3	-1815,5	-115,7	643,5
950	1000	975	52,6	1303,9	1097	-3629	-2531	57,7	2516,7	-190,8	-2006,3	-133,1	510,4
900	950	925	44,2	1348,1	915	-3959	-3044	40,4	2557,1	-174,9	-2181,2	-134,5	376,0
850	900	875	39,3	1387,4	696	-4212	-3515	27,4	2584,5	-165,6	-2346,7	-138,2	237,8
800	850	825	35,5	1422,9	476	-4432	-3955	16,9	2601,4	-157,1	-2503,9	-140,2	97,6
750	800	775	32,5	1455,4	258	-4727	-4469	8,4	2609,8	-153,5	-2657,3	-145,1	-47,5
700	750	725	26	1481,4	138	-5308	-5170	3,6	2613,4	-137,8	-2795,1	-134,2	-181,7
650	700	675	12,5	1493,9	80	-5879	-5799	1,0	2614,4	-73,6	-2868,7	-72,5	-254,3
600	650	625	1,1	1495,0	34	-6198	-6163	0,0	2614,4	-7,0	-2875,7	-7,0	-261,3

Eyjabakkajökull

Elevation (m a.s.l.)			ΔS (km^2)	∑ΔS (km^2)	b_w (mm)	b_s (mm)	b_n (mm)	ΔB_w ($10^6 m^3$)	$\sum\Delta B_w$ ($10^6 m^3$)	ΔB_s ($10^6 m^3$)	$\sum\Delta B_s$ ($10^6 m^3$)	ΔB_n ($10^6 m^3$)	$\sum B_n$ ($10^6 m^3$)
1550	1600	1575	0	0,0	3185	-835	2350	0,1	0,1	0,0	0,0	0,0	0,0
1500	1550	1525	0	0,0	3172	-839	2332	0,3	0,4	0,0	-0,1	0,2	0,3
1450	1500	1475	1,1	1,1	3129	-874	2255	3,6	4,0	-1,0	-1,1	2,6	2,9
1400	1450	1425	2,1	3,2	3073	-914	2158	6,3	10,4	-1,9	-3,0	4,4	7,4
1350	1400	1375	2,7	5,9	2948	-1028	1920	7,9	18,3	-2,8	-5,8	5,2	12,5
1300	1350	1325	4,5	10,4	2812	-1177	1634	12,7	31,0	-5,3	-11,1	7,4	19,9
1250	1300	1275	13,8	24,2	2465	-1377	1087	33,9	64,9	-19,0	-30,1	15,0	34,9
1200	1250	1225	13,3	37,5	2247	-1514	733	29,8	94,7	-20,1	-50,1	9,7	44,6
1150	1200	1175	14,2	51,7	2070	-1775	295	29,4	124,2	-25,2	-75,4	4,2	48,8
1100	1150	1125	11,7	63,4	1827	-2162	-335	21,3	145,5	-25,2	-100,6	-3,9	44,9
1050	1100	1075	10	73,4	1525	-2724	-1199	15,2	160,7	-27,2	-127,7	-12,0	32,9
1000	1050	1025	9,3	82,7	1263	-3344	-2081	11,8	172,4	-31,1	-158,9	-19,4	13,6
950	1000	975	7,5	90,2	1000	-3960	-2960	7,5	179,9	-29,7	-188,6	-22,2	-8,6
900	950	925	5	95,2	820	-4471	-3650	4,1	184,0	-22,3	-210,9	-18,2	-26,9
850	900	875	3,8	99,0	733	-4866	-4132	2,8	186,8	-18,6	-229,5	-15,8	-42,7
800	850	825	2,9	101,9	688	-5353	-4665	2,0	188,9	-15,7	-245,3	-13,7	-56,4
750	800	775	1,9	103,8	640	-6005	-5364	1,2	190,1	-11,7	-256,9	-10,4	-66,8
700	750	725	1,7	105,5	585	-6248	-5662	1,0	191,1	-10,9	-267,8	-9,9	-76,7
650	700	675	1	106,5	494	-6445	-5951	0,5	191,6	-6,6	-274,5	-6,1	-82,9

Hoffellsjökull

Elevation (m a.s.l.)			ΔS (km^2)	∑ΔS (km^2)	b_w (mm)	b_s (mm)	b_n (mm)	ΔB_w ($10^6 m^3$)	$\sum\Delta B_w$ ($10^6 m^3$)	ΔB_s ($10^6 m^3$)	$\sum\Delta B_s$ ($10^6 m^3$)	ΔB_n ($10^6 m^3$)	$\sum B_n$ ($10^6 m^3$)
1450	1500	1475	1,2	1,2	3139	-856	2283	3,7	3,7	-1,0	-1,0	2,7	2,7
1400	1450	1425	7,3	8,5	2801	-768	2033	20,5	24,2	-5,6	-6,6	14,9	17,6
1350	1400	1375	10,2	18,7	2692	-913	1778	27,4	51,6	-9,3	-15,9	18,1	35,7
1300	1350	1325	16,4	35,1	2522	-1089	1432	41,4	93,0	-17,9	-33,8	23,5	59,2
1250	1300	1275	34,9	70,0	2314	-1315	998	80,8	173,9	-45,9	-79,8	34,9	94,1
1200	1250	1225	25,6	95,6	2134	-1401	733	54,6	228,4	-35,8	-115,6	18,7	112,8
1150	1200	1175	17,9	113,5	1950	-1536	414	34,9	263,4	-27,5	-143,1	7,4	120,3
1100	1150	1125	16,7	130,2	1809	-1723	86	30,2	293,6	-28,8	-171,9	1,4	121,7
1050	1100	1075	12,5	142,7	1666	-1981	-314	20,9	314,4	-24,8	-196,7	-3,9	117,8
1000	1050	1025	9,7	152,4	1556	-2204	-647	15,0	329,5	-21,3	-218,0	-6,3	111,5
950	1000	975	8,6	161,0	1453	-2430	-977	12,5	341,9	-20,9	-238,8	-8,4	103,1
900	950	925	6,4	167,4	1363	-2701	-1337	8,7	350,6	-17,2	-256,0	-8,5	94,6
850	900	875	4,2	171,6	1289	-2969	-1680	5,4	356,0	-12,5	-268,5	-7,1	87,5
800	850	825	3,6	175,2	1255	-3190	-1935	4,6	360,6	-11,6	-280,2	-7,1	80,5
750	800	775	3,8	179,0	1213	-3342	-2129	4,6	365,2	-12,7	-292,9	-8,1	72,4
700	750	725	3,3	182,3	1097	-3680	-2583	3,6	368,9	-12,2	-305,1	-8,6	63,8
650	700	675	3,5	185,8	972	-4120	-3147	3,4	372,2	-14,3	-319,4	-11,0	52,9
600	650	625	2,5	188,3	890	-4486	-3595	2,2	374,5	-11,3	-330,7	-9,0	43,8
550	600	575	1,7	190,0	829	-4731	-3902	1,4	375,9	-7,9	-338,5	-6,5	37,4
500	550	525	1,5	191,5	756	-4992	-4235	1,1	377,0	-7,4	-345,9	-6,3	31,1
450	500	475	0,9	192,4	660	-5350	-4690	0,6	377,6	-4,9	-350,8	-4,3	26,8
400	450	425	0,7	193,1	578	-5663	-5084	0,4	378,0	-4,2	-355,0	-3,8	23,0
350	400	375	0,7	193,8	478	-6063	-5584	0,3	378,3	-4,1	-359,1	-3,7	19,3
300	350	325	0,5	194,3	376	-6407	-6030	0,2	378,5	-3,3	-362,4	-3,1	16,1
250	300	275	0,7	195,0	271	-6744	-6472	0,2	378,7	-5,0	-367,4	-4,8	11,3
200	250	225	1,5	196,5	146	-7334	-7188	0,2	379,0	-11,1	-378,5	-10,9	0,4
150	200	175	2,3	198,8	-13	-8039	-8053	0,0	378,9	-18,9	-397,4	-18,9	-18,5
100	150	125	2,5	201,3	-167	-8667	-8835	-0,4	378,5	-21,8	-419,3	-22,3	-40,8
50	100	75	1,9	203,2	-336	-9174	-9511	-0,6	377,9	-17,5	-436,8	-18,2	-58,9
0	50	25	2,2	205,4	-498	-9750	-10248	-1,1	376,8	-21,5	-458,3	-22,5	-81,5

Breiðamerkurjökull

Elevation (m a.s.l.)			ΔS (km^2)	∑ΔS (km^2)	b_w (mm)	b_s (mm)	b_n (mm)	ΔB_w ($10^6 m^3$)	$\sum\Delta B_w$ ($10^6 m^3$)	ΔB_s ($10^6 m^3$)	$\sum\Delta B_s$ ($10^6 m^3$)	ΔB_n ($10^6 m^3$)	$\sum B_n$ ($10^6 m^3$)
1900	1950	1925	0	0,0	5015	2526	7541	0,3	0,3	0,1	0,1	0,4	0,4
1850	1900	1875	0,4	0,4	4931	2325	7257	1,9	2,1	0,9	1,0	2,8	3,1
1800	1850	1825	0,5	0,9	4764	1945	6709	2,2	4,3	0,9	1,9	3,1	6,2
1750	1800	1775	0,9	1,8	4461	1410	5872	4,0	8,3	1,3	3,2	5,2	11,4
1700	1750	1725	2,6	4,4	3416	337	3754	9,1	17,3	0,9	4,1	9,9	21,4
1650	1700	1675	6,2	10,6	2839	-172	2666	17,5	34,8	-1,1	3,0	16,4	37,8
1600	1650	1625	17,7	28,3	2648	-418	2230	46,8	81,7	-7,4	-4,4	39,4	77,3
1550	1600	1575	26,2	54,5	2570	-638	1932	67,4	149,1	-16,7	-21,1	50,7	127,9
1500	1550	1525	32	86,5	2513	-845	1667	80,5	229,5	-27,1	-48,2	53,4	181,3
1450	1500	1475	46,4	132,9	2490	-927	1562	115,6	345,1	-43,1	-91,3	72,5	253,8
1400	1450	1425	58	190,9	2425	-1015	1410	140,8	485,9	-58,9	-150,2	81,9	335,7
1350	1400	1375	88,8	279,7	2351	-1213	1138	208,9	694,8	-107,8	-258,0	101,1	436,8
1300	1350	1325	95,3	375,0	2370	-1480	890	225,9	920,7	-141,1	-399,0	84,9	521,7
1250	1300	1275	57,4	432,4	2397	-1835	562	137,6	1058,3	-105,3	-504,4	32,3	553,9
1200	1250	1225	39,4	471,8	2330	-2125	204	91,9	1150,3	-83,9	-588,2	8,1	562,0
1150	1200	1175	31,8	503,6	2190	-2344	-153	69,8	1220,0	-74,6	-662,9	-4,9	557,1
1100	1150	1125	27	530,6	2011	-2522	-510	54,4	1274,4	-68,2	-731,0	-13,8	543,4
1050	1100	1075	23,8	554,4	1867	-2691	-824	44,4	1318,8	-64,0	-795,0	-19,6	523,7
1000	1050	1025	22,1	576,5	1768	-2858	-1090	39,2	1357,9	-63,3	-858,3	-24,1	499,6
950	1000	975	24,4	600,9	1655	-3076	-1421	40,4	1398,3	-75,0	-933,3	-34,7	464,9
900	950	925	26,6	627,5	1545	-3292	-1747	41,1	1439,4	-87,5	-1020,8	-46,4	418,5
850	900	875	23,7	651,2	1431	-3575	-2143	33,9	1473,2	-84,6	-1105,4	-50,7	367,8
800	850	825	24,3	675,5	1310	-3795	-2485	31,8	1505,0	-92,2	-1197,6	-60,3	307,5
750	800	775	25,4	700,9	1179	-4049	-2869	29,9	1535,0	-102,8	-1300,4	-72,9	234,6
700	750	725	20,3	721,2	1072	-4268	-3196	21,7	1556,7	-86,5	-1386,9	-64,8	169,8
650	700	675	30	751,2	972	-4469	-3496	29,2	1585,9	-134,0	-1520,9	-104,8	65,0
600	650	625	25,9	777,1	930	-4699	-3769	24,1	1610,0	-121,8	-1642,7	-97,7	-32,7
550	600	575	26,8	803,9	912	-5052	-4140	24,5	1634,5	-135,5	-1778,2	-111,1	-143,7
500	550	525	18	821,9	896	-5284	-4387	16,1	1650,6	-94,9	-1873,0	-78,8	-222,5
450	500	475	13,1	835,0	879	-5492	-4612	11,5	1662,1	-71,9	-1944,9	-60,4	-282,9
400	450	425	16,6	851,6	856	-5613	-4756	14,2	1676,3	-93,1	-2038,0	-78,9	-361,7
350	400	375	12,8	864,4	802	-5787	-4984	10,3	1686,5	-74,0	-2112,0	-63,7	-425,4
300	350	325	10,6	875,0	692	-6167	-5475	7,4	1693,9	-65,6	-2177,6	-58,3	-483,7
250	300	275	10,8	885,8	519	-6766	-6247	5,6	1699,5	-72,7	-2250,3	-67,2	-550,8
200	250	225	9,4	895,2	297	-7488	-7190	2,8	1702,3	-70,2	-2320,5	-67,4	-618,2
150	200	175	9,8	905,0	36	-8205	-8169	0,4	1702,6	-80,2	-2400,7	-79,9	-698,1
100	150	125	8,1	913,1	-231	-8887	-9119	-1,9	1700,8	-71,6	-2472,4	-73,5	-771,6
50	100	75	6,5	919,6	-408	-9643	-10052	-2,6	1698,1	-62,2	-2534,6	-64,8	-836,5
0	50	25	3	922,6	-505	-10190	-10695	-1,5	1696,6	-31,0	-2565,6	-32,5	-869,0

Síðujökull

Elevation (m a.s.l.)			ΔS (km^2)	∑ΔS (km^2)	b_w (mm)	b_s (mm)	b_n (mm)	ΔB_w ($10^6 m^3$)	$\sum\Delta B_w$ ($10^6 m^3$)	ΔB_s ($10^6 m^3$)	$\sum\Delta B_s$ ($10^6 m^3$)	ΔB_n ($10^6 m^3$)	$\sum B_n$ ($10^6 m^3$)
1700	1750	1725	0,9	0,9	1977	-170	1806	1,8	1,8	-0,2	-0,2	1,6	1,6
1650	1700	1675	5,9	6,8	1974	-352	1622	11,7	13,4	-2,1	-2,2	9,6	11,2
1600	1650	1625	11,2	18,0	1955	-425	1529	21,9	35,3	-4,8	-7,0	17,1	28,3
1550	1600	1575	11,5	29,5	1958	-511	1447	22,5	57,8	-5,9	-12,9	16,6	44,9
1500	1550	1525	21,3	50,8	1959	-624	1335	41,8	99,6	-13,3	-26,2	28,5	73,4
1450	1500	1475	38,2	89,0	1973	-802	1170	75,4	175,0	-30,6	-56,8	44,7	118,1
1400	1450	1425	24,9	113,9	1965	-929	1036	48,9	223,9	-23,1	-79,9	25,8	143,9
1350	1400	1375	21,1	135,0	1988	-1077	911	42,0	265,9	-22,8	-102,7	19,3	163,2
1300	1350	1325	17,2	152,2	2004	-1261	742	34,6	300,5	-21,8	-124,5	12,8	176,0
1250	1300	1275	15,6	167,8	2009	-1450	558	31,3	331,7	-22,6	-147,0	8,7	184,7
1200	1250	1225	21,2	189,0	2046	-1596	449	43,3	375,0	-33,8	-180,8	9,5	194,2
1150	1200	1175	17,9	206,9	2068	-1828	240	37,0	412,0	-32,7	-213,5	4,3	198,5
1100	1150	1125	17	223,9	2039	-2082	-42	34,6	446,6	-35,3	-248,8	-0,7	197,8
1050	1100	1075	15,4	239,3	1967	-2422	-454	30,4	477,0	-37,4	-286,2	-7,0	190,8
1000	1050	1025	19,3	258,6	1864	-2785	-920	36,0	513,0	-53,8	-340,1	-17,8	173,0
950	1000	975	19,8	278,4	1738	-3211	-1472	34,4	547,4	-63,6	-403,6	-29,2	143,8
900	950	925	20,3	298,7	1619	-3667	-2048	32,9	580,3	-74,4	-478,1	-41,6	102,2
850	900	875	19	317,7	1482	-4059	-2577	28,1	608,4	-77,0	-555,1	-48,9	53,3
800	850	825	18,8	336,5	1305	-4470	-3164	24,6	633,0	-84,1	-639,2	-59,6	-6,2
750	800	775	21,4	357,9	1067	-4930	-3863	22,8	655,8	-105,5	-744,7	-82,7	-88,9
700	750	725	21,5	379,4	794	-5319	-4525	17,1	672,9	-114,3	-859,0	-97,2	-186,1
650	700	675	20,6	400,0	613	-5691	-5078	12,7	685,5	-117,5	-976,5	-104,8	-290,9
600	650	625	9,7	409,7	511	-5986	-5474	5,0	690,5	-58,3	-1034,8	-53,3	-344,3
550	600	575	0,2	409,9	479	-6130	-5651	0,0	690,6	-1,1	-1035,9	-1,0	-345,3

Skaftárjökull

Elevation (m a.s.l.)			ΔS (km^2)	∑ΔS (km^2)	b_w (mm)	b_s (mm)	b_n (mm)	ΔB_w ($10^6 m^3$)	$\sum\Delta B_w$ ($10^6 m^3$)	ΔB_s ($10^6 m^3$)	$\sum\Delta B_s$ ($10^6 m^3$)	ΔB_n ($10^6 m^3$)	$\sum B_n$ ($10^6 m^3$)
1350	1400	1375	2,3	2,3	2135	-2535	-399	5,0	5,0	-5,9	-5,9	-0,9	-0,9
1300	1350	1325	5,4	7,7	1949	-2845	-896	10,4	15,4	-15,2	-21,2	-4,8	-5,7
1250	1300	1275	4,2	11,9	1831	-3195	-1363	7,8	23,2	-13,5	-34,7	-5,8	-11,5
1200	1250	1225	6,5	18,4	1728	-3532	-1803	11,2	34,4	-22,9	-57,6	-11,7	-23,2
1150	1200	1175	7,9	26,3	1609	-3765	-2156	12,7	47,1	-29,7	-87,3	-17,0	-40,2
1100	1150	1125	11,2	37,5	1467	-3863	-2396	16,4	63,4	-43,1	-130,4	-26,7	-66,9
1050	1100	1075	12,9	50,4	1283	-3967	-2683	16,6	80,0	-51,3	-181,6	-34,7	-101,6
1000	1050	1025	12,9	63,3	1092	-4354	-3262	14,1	94,2	-56,4	-238,0	-42,2	-143,8
950	1000	975	8,5	71,8	877	-4832	-3954	7,5	101,6	-41,2	-279,1	-33,7	-177,5
900	950	925	5,5	77,3	697	-5175	-4478	3,8	105,5	-28,3	-307,4	-24,5	-202,0
850	900	875	5,3	82,6	517	-5474	-4956	2,8	108,2	-29,2	-336,7	-26,5	-228,5
800	850	825	5,0	87,6	339	-5774	-5434	1,7	109,9	-28,6	-365,3	-26,9	-255,4
750	800	775	4,6	92,2	157	-6028	-5871	0,7	110,6	-28,0	-393,2	-27,2	-282,6
700	750	725	4,3	96,5	-23	-6426	-6450	-0,1	110,5	-27,4	-420,7	-27,5	-310,1
650	700	675	1,6	98,1	-165	-6854	-7020	-0,3	110,3	-11,0	-431,6	-11,2	-321,4
600	650	625	0,0	98,1	-262	-7643	-7905	0,0	110,3	0,0	-431,7	0,0	-321,5

Vestari Skaftárketill

Elevation (m a.s.l.)			ΔS (km^2)	∑ΔS (km^2)	b_w (mm)	b_s (mm)	b_n (mm)	ΔB_w ($10^6 m^3$)	$\sum\Delta B_w$ ($10^6 m^3$)	ΔB_s ($10^6 m^3$)	$\sum\Delta B_s$ ($10^6 m^3$)	ΔB_n ($10^6 m^3$)	$\sum B_n$ ($10^6 m^3$)
1900	1950	1925	0,6	0,6	2233	258	2492	1,3	1,3	0,1	0,1	1,4	1,4
1850	1900	1875	0,6	1,2	2207	197	2405	1,4	2,6	0,1	0,3	1,5	2,9
1800	1850	1825	0,8	2,0	2170	111	2282	1,7	4,3	0,0	0,4	1,8	4,7
1750	1800	1775	2,6	4,6	2082	-99	1982	5,2	9,5	-0,2	0,1	4,9	9,6
1700	1750	1725	5,5	10,1	1975	-252	1722	10,7	20,2	-1,4	-1,3	9,3	19,0
1650	1700	1675	6,6	16,7	1865	-381	1483	12,1	32,3	-2,5	-3,7	9,6	28,6
1600	1650	1625	7,6	24,3	1819	-472	1347	13,1	45,4	-3,4	-7,1	9,7	38,2
1550	1600	1575	5,5	29,8	1781	-560	1220	8,9	54,3	-2,8	-9,9	6,1	44,4
1500	1550	1525	1,5	31,3	1750	-618	1131	4,7	59,0	-1,7	-11,6	3,0	47,4

Eystri Skaftárketill

Elevation (m a.s.l.)			ΔS (km^2)	∑ΔS (km^2)	b_w (mm)	b_s (mm)	b_n (mm)	ΔB_w ($10^6 m^3$)	$\sum\Delta B_w$ ($10^6 m^3$)	ΔB_s ($10^6 m^3$)	$\sum\Delta B_s$ ($10^6 m^3$)	ΔB_n ($10^6 m^3$)	$\sum B_n$ ($10^6 m^3$)
1750	1800	1775	1,1	1,1	2051	-202	1848	2,3	2,3	-0,2	-0,2	2,0	2,0
1700	1750	1725	10,2	11,3	1980	-293	1687	19,4	21,7	-2,9	-3,1	16,6	18,6
1650	1700	1675	16,5	27,8	1919	-331	1588	29,7	51,4	-5,1	-8,2	24,6	43,2
1600	1650	1625	9,7	37,5	1888	-365	1523	17,5	68,9	-3,4	-11,6	14,1	57,3
1550	1600	1575	2,4	39,9	1880	-389	1491	8,0	76,8	-1,7	-13,3	6,3	63,6

Gjálp

Elevation (m a.s.l.)			ΔS (km^2)	∑ΔS (km^2)	b_w (mm)	b_s (mm)	b_n (mm)	ΔB_w ($10^6 m^3$)	$\sum\Delta B_w$ ($10^6 m^3$)	ΔB_s ($10^6 m^3$)	$\sum\Delta B_s$ ($10^6 m^3$)	ΔB_n ($10^6 m^3$)	$\sum B_n$ ($10^6 m^3$)
1900	1950	1925	0,4	0,4	2247	261	2508	0,8	0,8	0,0	0,0	0,9	0,9
1850	1900	1875	0,7	1,1	2206	158	2365	1,6	2,4	0,1	0,2	1,8	2,6
1800	1850	1825	1,1	2,2	2148	11	2160	2,5	4,9	0,0	0,2	2,5	5,2
1750	1800	1775	4,9	7,1	2055	-220	1835	11,3	16,2	-1,2	-1,0	10,1	15,2
1700	1750	1725	18,8	25,9	2004	-314	1690	47,1	63,3	-7,4	-8,4	39,7	55,0
1650	1700	1675	13,5	39,4	1970	-312	1657	16,0	79,3	-2,5	-10,9	13,4	68,4

Grímsvötn

Elevation (m a.s.l.)			ΔS (km^2)	∑ΔS (km^2)	b_w (mm)	b_s (mm)	b_n (mm)	ΔB_w ($10^6 m^3$)	$\sum\Delta B_w$ ($10^6 m^3$)	ΔB_s ($10^6 m^3$)	$\sum\Delta B_s$ ($10^6 m^3$)	ΔB_n ($10^6 m^3$)	$\sum B_n$ ($10^6 m^3$)
1700	1750	1725	1,4	1,4	1969	-322	1647	2,7	2,7	-0,4	-0,4	2,3	2,3
1650	1700	1675	41	42,4	1943	-335	1608	79,7	82,4	-13,7	-14,2	66,0	68,2
1600	1650	1625	30,9	73,3	1926	-414	1512	59,5	141,9	-12,8	-27,0	46,7	114,9
1550	1600	1575	20	93,3	2017	-624	1392	40,4	182,3	-12,5	-39,5	27,9	142,8
1500	1550	1525	16,8	110,1	2099	-1092	1006	35,2	217,4	-18,3	-57,8	16,9	159,6
1450	1500	1475	9,7	119,8	2111	-1421	690	20,5	238,0	-13,8	-71,6	6,7	166,4
1400	1450	1425	13,8	133,6	2136	-1562	574	29,5	267,5	-21,6	-93,2	7,9	174,3
1350	1400	1375	1,5	135,1	2087	-1449	637	3,2	270,7	-2,2	-95,4	1,0	175,3

Appendix C: Coordinates of the velocity measurement stakes in 2020.

Position of the velocity measurement stakes determined by GPS sub-metre differential (I), fast static (FS) and kinematic (K). (Accuracy of horizontal position 0.5 – 1.0 m, and vertical accuracy 1-2 m for DGPS, about 1cm for fast static, and 3 cm for kinematic).
The station Hofn in Höfn í Hornafirði is used as a stationary reference for all measurements, ÍSN93 datum, h_l is elevation above ellipsoid, dL antenna height, N estimated difference between ellipsoid and sea-level, H elevation in metres above sea level ($H= h_l+N+dL$). X and Y are ÍSN93 Lambert conformal conic projected coordinates. M is a quality marker.

Site	time	Date	Calender Day #	Year	Latitude		Longitude		h_l (m a. e.)	dL (m)	N (m)	H (m a. s. l.)	X	Y	M
B07-20	21,244	4	6	156	2020	64	25,7966	16	17,4682	1427,4	-1,6	-67,1	1358,8	630464,3	439245,4	K
B07-20	10,236	9	10	283	2020	64	25,7957	16	17,4674	1422,6	0	-67,1	1355,5	630465,1	439243,8	K
B09-20	16,341	30	4	121	2020	64	44,8344	16	5,8532	786,84	0	-66,7	720,17	638157,9	474994,1	K
B09-20	13,365	9	10	283	2020	64	44,8352	16	5,85493	780,78	0	-66,7	714,11	638156,5	474995,4	K
B10-19	16,557	30	4	121	2020	64	43,6871	16	6,69886	841,28	0	-66,7	774,57	637584,9	472833,9	K
B10-20	17,643	30	4	121	2020	64	43,6871	16	6,69798	841,14	0	-66,7	774,44	637585,6	472833,9	K
B10-20	14,498	9	10	283	2020	64	43,6873	16	6,69778	836,06	0	-66,7	769,35	637585,7	472834,2	K
B11-20	18,922	30	4	121	2020	64	40,936	16	10,4688	1017,9	0	-66,8	951,05	634822,3	467592,1	K
B11-20	12,291	9	10	283	2020	64	40,9407	16	10,4655	1013,7	0	-66,8	946,88	634824,5	467601,1	K
B12-20	18,943	30	4	121	2020	64	38,2673	16	14,1395	1145,4	0	-66,9	1078,5	632121,8	462509,3	K
B12-20	11,676	9	10	283	2020	64	38,2777	16	14,1309	1142,3	0	-66,9	1075,4	632127,8	462529	K
B13-19	11,881	9	10	283	2020	64	34,5603	16	19,6694	1286,6	0	-67	1219,6	628010,4	455438,5	K
B13-20	13,964	1	5	122	2020	64	34,5777	16	19,6424	1287,9	0	-67	1220,9	628030,6	455471,7	K
B13-20	11,755	9	10	283	2020	64	34,5913	16	19,6268	1285,6	0	-67	1218,5	628042	455497,6	K
B13ror15	10,511	9	10	283	2020	64	34,6229	16	19,6126	1286,4	0	-67	1219,3	628050,9	455556,6	K
B14-20	13	30	4	121	2020	64	31,6407	16	24,702	1387,8	0	-67,1	1320,6	624216,6	449851,2	O
B14-20	12,509	9	10	283	2020	64	31,6516	16	24,6862	1385,9	0	-67,1	1318,8	624228,5	449872	K
B15-20	12	30	4	121	2020	64	28,4924	16	30,0268	1472,4	-1,6	-67,2	1403,6	620191,1	443835	K
B15-20	12,196	9	10	283	2020	64	28,4974	16	30,0147	1468,9	0	-67,2	1401,6	620200,4	443844,7	K
B16-20	18,05	1	5	122	2020	64	24,1269	16	40,8871	1597,7	0	-67,3	1530,3	611788,9	435397,6	K
B16-20	15,504	9	10	283	2020	64	24,1274	16	40,8863	1593,3	0	-67,3	1525,9	611789,5	435398,6	K
B17-20	19,804	30	4	121	2020	64	36,7316	16	28,795	1285,6	0	-67,1	1218,5	620567,6	459170,4	K
B17-20	12,966	9	10	283	2020	64	36,7447	16	28,7871	1282,1	0	-67,1	1215	620573	459194,9	K
B18-20	13,063	29	4	120	2020	64	31,5604	16	0,12554	1383,9	0	-66,9	1317	643867,7	450570,8	K
B18-20	15,219	8	10	282	2020	64	31,5662	16	0,12865	1379,8	0	-66,9	1312,9	643864,7	450581,5	K
B19-20	11,611	29	4	120	2020	64	27,9947	15	55,9898	1507,3	0	-66,9	1440,4	647494,2	444112,2	K
B19-20	14,143	8	10	282	2020	64	27,9954	15	55,9902	1503,1	0	-66,9	1436,2	647493,9	444113,5	K
BB0-20	9,751	29	4	120	2020	64	22,7094	16	5,05338	1586,7	0	-66,9	1519,8	640687,4	433958,7	K
BB0-20	13,487	8	10	282	2020	64	22,7098	16	5,05461	1582,6	0	-66,9	1515,7	640686,4	433959,4	K
BB06-20	17,067	3	6	155	2020	64	36,6572	17	27,5185	1978	0	-67,9	1910,2	573758,3	457528,5	K
BB07-20	17,58	3	6	155	2020	64	36,0953	17	27,5285	1975,7	0	-67,9	1907,8	573775,8	456484,1	K
BB08-20	16,716	3	6	155	2020	64	37,1635	17	29,5622	1988,1	0	-67,9	1920,2	572106,3	458429,1	K
BB09-20	16,497	3	6	155	2020	64	36,5111	17	30,5588	1980,7	0	-67,9	1912,9	571340,4	457198,3	K
BB11-20	16,347	3	6	155	2020	64	36,0721	17	31,4069	1958,6	0	-67,9	1890,7	570683,1	456367	K
BB12-20	16,116	3	6	155	2020	64	36,5584	17	34,5458	1960,3	0	-67,9	1892,4	568158,9	457212,9	K
BB13-20	15,984	3	6	155	2020	64	37,2343	17	32,6343	1998,5	0	-67,9	1930,6	569654,3	458503,2	K
BB14-20	15,661	3	6	155	2020	64	38,1779	17	32,5719	2020,7	0	-67,9	1952,9	569663,7	460257	K
BB15-20	15,825	3	6	155	2020	64	38,0808	17	30,5109	1999,7	0	-67,9	1931,8	571309,8	460115	K
BB16-20	14,915	3	6	155	2020	64	39,1349	17	30,5434	2009,6	0	-67,9	1941,7	571237,7	462072,3	K
BB17-20	14,744	3	6	155	2020	64	38,5614	17	28,8281	1985,6	0	-67,9	1917,7	572629,1	461039,7	K
BB18-20	12,904	3	6	155	2020	64	39,539	17	26,7056	1962,7	0	-67,9	1894,9	574274,8	462896,5	K
BB19-20	13,525	3	6	155	2020	64	39,1056	17	22,8757	1929,9	0	-67,8	1862,1	577343,9	462168	K
BB20-20	13,377	3	6	155	2020	64	38,9504	17	23,528	1941,3	0	-67,9	1873,5	576832	461866,5	K
BB21-20	14,415	3	6	155	2020	64	38,6886	17	24,7737	1945,8	0	-67,9	1877,9	575852,2	461355,3	K
BB22-20	14,534	3	6	155	2020	64	38,4186	17	25,646	1953,1	0	-67,9	1885,2	575170	460836,3	K
BB23a-20	16,814	3	6	155	2020	64	37,6812	17	27,5694	1972,7	0	-67,9	1904,8	573671,4	459428,9	K
BB23b-20	16,971	3	6	155	2020	64	37,1362	17	27,5288	1973,1	0	-67,9	1905,3	573728,4	458417,4	K

BB24-20	17,255	3	6	155	2020	64	37,1728	17	24,5807	1937	0	-67,9	1869,2	576076,8	458543,6	K
BB25-20	13,857	3	6	155	2020	64	38,0001	17	21,3983	1874,9	0	-67,8	1807,1	578573,6	460145,1	K
BB26-20	14,167	3	6	155	2020	64	37,6146	17	20,5463	1841,3	0	-67,8	1773,5	579271,2	459446,8	K
BB30-20	11,041	3	6	155	2020	64	39,9927	17	14,5929	1567,2	0	-67,7	1499,5	583892,4	463991,8	K
BB31-20	11,419	3	6	155	2020	64	42,0381	17	15,2296	1531,3	0	-67,6	1463,7	583280,8	467776,6	K
BB32-20	12,19	3	6	155	2020	64	43,1123	17	19,947	1570,5	0	-67,7	1502,8	579479,3	469670,5	K
BB34-20	12,412	3	6	155	2020	64	42,0541	17	21,3072	1626,8	0	-67,8	1559	578450,2	467676,8	K
BB35-20	11,616	3	6	155	2020	64	40,987	17	18,1151	1606,8	0	-67,7	1539,1	581040,2	465761,8	K
BB36-20	11,848	3	6	155	2020	64	40,1345	17	20,2608	1719,2	0	-67,8	1651,4	579375,5	464133,1	K
BB39-20	17,672	3	6	155	2020	64	35,5657	17	27,6315	1901,8	0	-67,9	1833,9	573717,7	455498,3	K
BB40-20	17,814	3	6	155	2020	64	35,1729	17	27,6664	1864,2	0	-67,9	1796,4	573707,6	454768,1	K
BB41-20	18,296	3	6	155	2020	64	34,1182	17	27,6993	1827,8	0	-67,9	1759,9	573729	452808,3	K
BB43-20	19,216	3	6	155	2020	64	34,9421	17	32,8205	1824,9	0	-67,9	1757	569603,8	454242	K
BB44-20	19,308	3	6	155	2020	64	34,7046	17	34,4988	1790,4	0	-67,8	1722,5	568274	453770,3	K
BB45-20	19,439	3	6	155	2020	64	34,0777	17	35,9997	1742,1	0	-67,8	1674,3	567101,5	452579	K
BB46a-20	19,718	3	6	155	2020	64	33,5836	17	38,4366	1685,7	0	-67,8	1617,9	565174,9	451618,6	K
BB46b-20	19,572	3	6	155	2020	64	33,5389	17	36,6021	1727,8	0	-67,8	1660	566642,3	451567,5	K
BB47-20	18,494	3	6	155	2020	64	32,9036	17	27,8114	1800,8	0	-67,8	1732,9	573694,3	450550,1	K
BB48-20	15,093	3	6	155	2020	64	39,8883	17	30,4799	2034,8	0	-67,9	1967	571255,3	463472,9	K
BB49-20	15,255	3	6	155	2020	64	39,1996	17	32,4764	2064,7	0	-67,9	1996,8	569695,9	462156,6	K
BB51-20	15,44	3	6	155	2020	64	38,091	17	34,774	1993,2	0	-67,9	1925,4	567912,9	460055,6	K
BB52-20	17,361	3	6	155	2020	64	36,6386	17	23,6339	1917,7	0	-67,9	1849,9	576856,7	457570,5	K
Barc-20	12,685	3	5	124	2020	64	38,4148	17	26,7664	1966,9	0	-67,9	1899	574277,8	460807,3	K
Barc-20	13,415	10	10	284	2020	64	38,4148	17	26,7598	1965,4	0	-67,9	1897,5	574283,1	460807,4	K
Bor-20	19,476	3	5	124	2020	64	24,9372	17	20,1473	1509,5	0	-67,7	1441,8	580209,1	435908,8	K
Bor-20	17,694	12	10	286	2020	64	24,9279	17	20,1493	1517,2	0	-67,7	1449,5	580208	435891,5	K
Borth-20	18,946	12	10	286	2020	64	25,0159	17	19,1915	1522,2	0	-67,7	1454,5	580972,9	436075,3	K
Br1-20	12,527	27	3	86	2020	64	5,96256	16	19,8204	180,93	-0,2	-65,9	114,9	630133	402345,5	K
Br1-20	14,319	13	8	226	2020	64	5,96194	16	19,8191	173,89	-1,05	-65,9	106,94	630134,3	402344,8	K
Br1-20	14,333	25	11	330	2020	64	5,96218	16	19,8201	169,37	-0,3	-65,9	103,17	630133,5	402345,2	K
Br2-19	13	27	3	86	2020	64	6,35947	16	22,5311	251,3	0	-66	185,27	627901,4	402991,4	K
Br2-20	13	27	3	86	2020	64	6,35947	16	22,5311	251,3	0	-66	185,27	627901,4	402991,4	K
Br2-20	10,667	25	11	330	2020	64	6,35916	16	22,5302	240,53	-0,3	-66	174,2	627902,4	402989,9	K
Br3-20	12,194	28	2	87	2020	64	8,44273	16	24,0155	437,97	-1,6	-66,3	370,1	626537,5	406808,2	K
Br3-20	12,383	25	11	330	2020	64	8,43642	16	24,0042	430,38	-0,3	-66,3	363,82	626547,1	406796,8	K
Br5-19	13,3	28	3	87	2020	64	13,3995	16	19,2282	732,58	-1,6	-66,6	664,44	630028,4	416171,8	K
Br5-20	10,477	5	5	126	2020	64	13,5316	16	19,2052	741,24	0	-66,6	674,68	630036,6	416418	K
Br7-20	9,889	5	5	126	2020	64	22,1367	16	16,9221	1314,1	0	-67	1247,1	631194,7	432470,4	K
Br7-20	11,661	9	10	283	2020	64	22,1106	16	16,9155	1308,7	0	-67	1241,7	631202,1	432422,2	K
Bru-20	9	30	4	121	2020	64	39,7487	15	56,5467	964,99	0	-66,8	898,21	645992,4	465904	O
Bru-20	18,882	8	10	282	2020	64	39,7562	15	56,5409	959,11	0	-66,8	892,33	645996,3	465918	K
Bud-20	10	30	4	121	2020	64	35,9956	15	59,8863	1210,5	0	-66,9	1143,7	643667,8	458811,1	O
Bud-20	19,234	8	10	282	2020	64	36,0051	15	59,8822	1201,2	0	-66,9	1134,3	643670,2	458829	K
D05-20	15,533	2	5	123	2020	64	42,2242	16	54,686	1272,8	0	-67,4	1205,5	599593,8	468617,6	K
D05-20	18,878	10	10	284	2020	64	42,2358	16	54,6696	1269,2	0	-67,4	1201,9	599606,2	468639,4	K
D06GPS20	18,041	10	10	284	2020	64	40,4513	16	56,9124	1338,9	-2	-67,4	1269,5	597931,9	465267,3	K
D07-20	13,095	2	5	123	2020	64	38,2837	16	59,2504	1445,7	0	-67,5	1377,8	596200,6	461182,1	K
D07-20	17,371	10	10	284	2020	64	38,299	16	59,2358	1442,2	0	-67,5	1374,7	596211,3	461210,9	K
D09-20	12,041	2	5	123	2020	64	31,7859	17	0,5942	1655,3	0	-67,6	1587,7	595510,3	449081,2	K
D09-20	20,526	10	10	284	2020	64	31,7898	17	0,59528	1652,7	0	-67,6	1585,2	595509,2	449088,5	K
D12-20	11,277	2	5	123	2020	64	28,9722	17	0,17817	1718,2	0	-67,6	1650,6	596008,1	443866,6	K
D12-20	21,034	10	10	284	2020	64	28,973	17	0,17786	1715,5	0	-67,6	1647,9	596008,3	443868	K
E01-20	18,334	29	4	120	2020	64	40,6362	15	34,8451	829,18	0	-66,7	762,46	663157,5	468435	K
E01-20	16,939	8	10	282	2020	64	40,6403	15	34,842	824,04	0	-66,7	757,32	663159,5	468442,9	K
E02-20	17,15	29	4	120	2020	64	39,1225	15	35,9877	1019,3	0	-66,8	952,52	662400,8	465577,7	K
E02-20	15,487	8	10	282	2020	64	39,1345	15	35,9849	1014,4	0	-66,8	947,63	662401,9	465600,1	K
E03-20	20,04	29	4	120	2020	64	36,6583	15	36,8996	1257,1	0	-66,9	1190,3	661920,7	460966,8	K
E03-20	18,25	8	10	282	2020	64	36,6637	15	36,9034	1251,6	0	-66,9	1184,8	661917,1	460976,6	K
E04-20	15,08	29	4	120	2020	64	34,9514	15	37,1458	1357	0	-66,8	1290,2	661894,1	457789,5	K
E04-20	14,996	8	10	282	2020	64	34,9524	15	37,1455	1352,4	0	-66,8	1285,5	661894,2	457791,3	K
E07-20	15,666	29	4	120	2020	64	38,4011	15	24,7038	1141,6	0	-66,6	1075	671449,8	464736	K
E07-20	14,298	13	10	287	2020	64	38,4058	15	24,6964	1136,3	0	-66,6	1069,7	671455,3	464745,1	K
E07a-20	11,534	29	4	120	2020	64	38,4118	15	24,834	1143,3	0	-66,6	1076,7	671345,2	464750	K
E07b-20	11,618	29	4	120	2020	64	38,4079	15	24,7337	1141,9	0	-66,6	1075,3	671425,4	464747,3	K
E07c-20	12,502	29	4	120	2020	64	38,3963	15	24,7003	1141,8	0	-66,6	1075,2	671453,1	464727,3	K
E07f-20	12,705	29	4	120	2020	64	38,4173	15	24,6857	1140,4	0	-66,6	1073,7	671462,5	464766,9	K

E07e-20	12,645	29	4	120	2020	64	38,4052	15	24,6751	1140,9	0	-66,6	1074,3	671472,2	464744,8	K
E08-20	16,417	29	4	120	2020	64	39,7158	15	23,8484	1021,2	0	-66,6	954,62	671991,2	467213,4	K
E08-20	13,793	13	10	287	2020	64	39,7179	15	23,8473	1016,4	0	-66,6	949,82	671991,9	467217,4	K
E09-20	17,432	29	4	120	2020	64	39,9893	15	28,2674	1049,1	0	-66,6	981,44	668450,3	467522,5	K
E09-20	13,493	13	10	287	2020	64	39,9897	15	28,2671	1044,2	0	-66,6	977,53	668450,6	467523,3	K
Fl01-20	10,881	29	4	120	2020	64	26,1558	15	55,6279	1415,6	0	-66,8	1348,8	647950,1	440713,7	K
Fl01-20	13,876	8	10	282	2020	64	26,1499	15	55,613	1410,5	0	-66,8	1343,7	647962,6	440703,3	K
G02-20	18,448	2	5	123	2020	64	26,8585	17	17,7141	1635,9	0	-67,7	1568,2	582066,9	439529,4	K
G02-20	9,376	12	10	286	2020	64	26,8544	17	17,7175	1633,1	0	-67,7	1565,4	582064,4	439521,7	K
G03-20	17,657	2	5	123	2020	64	28,4364	17	16,3288	1728,6	0	-67,7	1660,9	583098	442490,1	K
G03-20	9,616	12	10	286	2020	64	28,4347	17	16,3297	1726,2	0	-67,7	1658,5	583097,4	442487	K
G04-20	16,93	2	5	123	2020	64	30,0229	17	15,0295	1757,6	0	-67,7	1689,9	584057,7	445465,3	K
G04-20	9,832	12	10	286	2020	64	30,0237	17	15,0285	1755,1	0	-67,7	1687,4	584058,4	445466,8	K
Go1-20	10,637	3	5	124	2020	64	33,9706	17	24,9438	1829,5	0	-67,8	1761,6	575936,4	452588,6	K
Go1-20	12,564	10	10	284	2020	64	33,9696	17	24,9431	1827,3	0	-67,8	1759,5	575937	452586,7	K
Haab-20	18,871	3	5	124	2020	64	20,9569	17	24,1197	1799,5	0	-67,5	1732	577205,8	428433,4	K
Haab-20	15,123	10	10	284	2020	64	20,9574	17	24,1199	1796,7	0	-67,5	1729,2	577205,7	428434,3	K
Hof01-20	14,31	29	4	120	2020	64	32,3361	15	35,8359	1210,1	0	-66,7	1143,4	663199,9	452993,3	K
Hof01-20	14,737	8	10	282	2020	64	32,3299	15	35,8355	1205,6	0	-66,7	1138,9	663200,8	452981,8	K
K01-20	11,851	3	5	124	2020	64	35,1667	17	51,8313	1115,4	0	-67,6	1047,8	554420	454348,3	K
K01-20	12,183	12	10	286	2020	64	35,1682	17	51,8367	1110,5	0	-67,6	1042,9	554415,6	454351,1	K
K02-20	12,052	3	5	124	2020	64	34,8091	17	49,6875	1239,1	0	-67,6	1171,4	556143,5	453715,3	K
K02-20	11,994	12	10	286	2020	64	34,8122	17	49,7015	1234,8	0	-67,6	1167,2	556132,2	453720,8	K
K03-20	12,54	3	5	124	2020	64	34,2381	17	46,3986	1362,2	0	-67,7	1294,5	558789,9	452704,4	K
K03-20	11,373	12	10	286	2020	64	34,241	17	46,4173	1358,2	0	-67,7	1290,5	558774,9	452709,5	K
K04-20	13,351	3	5	124	2020	64	33,2119	17	42,2525	1555,4	0	-67,7	1487,7	562140,3	450864,2	K
K04-20	10,818	12	10	286	2020	64	33,2158	17	42,2768	1551,2	0	-67,7	1483,5	562120,7	450871,1	K
K05-20	15,739	3	5	124	2020	64	33,4462	17	35,4567	1748,3	0	-67,8	1680,5	567561,3	451415,7	K
K05-20	10,389	12	10	286	2020	64	33,444	17	35,4705	1745,1	0	-67,8	1677,2	567550,4	451411,4	K
K06-20	14,405	3	5	124	2020	64	38,3556	17	31,3207	2014,7	0	-67,9	1946,8	570652,7	460610,3	K
K06-20	14,234	10	10	284	2020	64	38,3551	17	31,3175	2012	0	-67,9	1944,2	570655,3	460609,4	K
K07-20	16,502	3	5	124	2020	64	29,1062	17	42,0344	1601,1	0	-67,7	1533,4	562471,4	443241	K
K07-20	13,048	12	10	286	2020	64	29,1067	17	42,0359	1598	0	-67,7	1530,3	562470,2	443241,9	K
Oer01-20	12,551	2	5	123	2020	63	59,8757	16	38,9931	1894,4	0	-66,3	1828	614984,9	390425,5	K
S01-20	16,729	3	5	124	2020	64	7,01496	17	49,9749	781,98	0	-66,8	715,14	556867,4	402078	K
S01-20	17,116	10	10	284	2020	64	7,01455	17	49,9759	775,83	0	-66,8	708,99	556866,6	402077,3	K
S02-20	16,119	3	5	124	2020	64	12,1596	17	48,9824	1070,3	0	-67,1	1003,3	557494,4	411650,3	K
S02-20	16,601	10	10	284	2020	64	12,1492	17	48,9873	1065,7	0	-67	998,61	557490,8	411630,8	K
S04-20	15,539	3	5	124	2020	64	16,1768	17	48,1899	1225,6	0	-67,2	1158,4	557994,5	419125,1	K
S04-20	16,18	10	10	284	2020	64	16,1629	17	48,2052	1221,4	0	-67,2	1154,2	557982,7	419099,1	K
S05-20	14,75	3	5	124	2020	64	20,5123	17	34,0025	1519,4	0	-67,5	1451,9	569268	427416,8	K
S05-20	15,458	10	10	284	2020	64	20,511	17	34,0173	1516	0	-67,5	1448,5	569256,2	427414,1	K
Ske02-20	17,756	1	5	122	2020	64	15,9093	17	0,0517	1249,5	0	-67,1	1182,5	596876,8	419611	K
Ske02-20	10,819	10	10	284	2020	64	15,8583	17	0,17032	1241,5	0	-67,1	1174,4	596784	419513,1	K
Ske03-20	19,845	1	5	122	2020	64	18,0586	16	56,1563	1369	0	-67,2	1301,8	599891,5	423703,3	K
Ske03-20	11,923	10	10	284	2020	64	18,0338	16	56,22	1362,6	0	-67,2	1295,4	599841,6	423655,7	K
Ske04-20	15,398	1	5	122	2020	64	20,1356	16	51,817	1468,5	0	-67,3	1401,2	603259,9	427676,5	K
Ske04-20	12,221	10	10	284	2020	64	20,1251	16	51,8464	1464,8	0	-67,3	1397,5	603236,9	427656,2	K
Ske05-20	14,69	1	5	122	2020	64	22,2321	16	47,2351	1543,1	0	-67,4	1475,7	606813,1	431696,4	K
Ske05-20	12,489	10	10	284	2020	64	22,2274	16	47,2464	1538,9	0	-67,4	1471,6	606804,3	431687,4	K
Skf00-20	18,925	28	4	119	2020	64	15,475	15	54,0832	1015,2	0	-66	949,13	650161	420953	K
Skf00-20	12,209	8	10	282	2020	64	15,4774	15	54,0799	1009,4	0	-66	943,32	650163,5	420957,5	K
Skf01-20	20,532	28	4	119	2020	64	18,0083	16	4,99962	1351,4	0	-66,6	1284,8	641133,4	425235,4	K
Skf01-20	13,125	8	10	282	2020	64	18,0062	16	4,98474	1347	0	-66,6	1280,4	641145,6	425232	K
T01-20	13,865	4	5	125	2020	64	19,4751	18	4,57078	959,55	0	-67,3	892,29	544676,7	425030,8	K
T01-20	15,765	12	10	286	2020	64	19,4757	18	4,57556	954,58	0	-67,3	887,32	544672,9	425031,8	K
T03-20	15,521	4	5	125	2020	64	20,2038	17	58,5835	1135,8	0	-67,3	1068,5	549480,3	426458,8	K
T03-20	14,426	12	10	286	2020	64	20,2023	17	58,5958	1132	0	-67,3	1064,7	549470,4	426455,9	K
T04-20	14,14	4	5	125	2020	64	21,3313	17	51,5132	1289,5	0	-67,4	1222,2	555138	428651,1	K
T04-20	13,436	12	10	286	2020	64	21,3282	17	51,5258	1285,8	0	-67,4	1218,4	555128	428645	K
T05-20	15,208	4	5	125	2020	64	22,2696	17	42,9877	1414,2	0	-67,5	1346,7	561965,5	430525,7	K
T05-20	12,752	12	10	286	2020	64	22,2668	17	42,9999	1410,7	0	-67,5	1343,3	561955,8	430520,3	K
T06-20	17,076	4	5	125	2020	64	24,2681	17	36,5171	1537,1	0	-67,6	1469,4	567089,4	434348,1	K
T06-20	11,594	12	10	286	2020	64	24,2646	17	36,5282	1533,4	0	-67,6	1465,8	567080,6	434341,4	K
T07-20	17,351	4	5	125	2020	64	25,296	17	31,2045	1632,6	0	-67,7	1564,9	571313,3	436354,3	K
T07-20	11,055	12	10	286	2020	64	25,2943	17	31,2127	1629,4	0	-67,7	1561,7	571306,7	436351,1	K
T08-20	18,308	3	5	124	2020	64	26,2939	17	27,7547	1705,6	0	-67,8	1637,8	574038,3	438274,1	K
T08-20	11,373	10	10	284	2020	64	26,2939	17	27,7564	1703,3	0	-67,8	1635,5	574036,9	438274,1	K

Appendix D: Measured surface velocity at marked sites on Vatnajökull in 2020.

Site	Calendar day date	#	Calendar day date	#	# of days	translation (m)	(°)	velocity (cm/day)	(m/annum)
B07-20	200604	156	201009	283	127	1,75	157	1,38	5,02
B09-20	200430	121	201009	283	162	1,93	315	1,19	4,34
B10-19	191019	292	200430	121	194	0,92	150	0,47	1,73
B10-20	200430	121	201009	283	162	0,4	23	0,25	0,91
B11-20	200430	121	201009	283	162	9,18	16	5,67	20,69
B12-20	200430	121	201009	283	162	20,56	19	12,69	46,33
B13-19	191019	292	201009	283	356	36,47	28	10,24	37,39
B13-20	200501	122	201009	283	161	28,18	26	17,51	63,89
B13ror15	191019	292	201009	283	356	35,8	29	10,06	36,7
B14-20	200430	121	201009	283	162	23,86	32	14,73	53,77
B15-20	200430	121	201009	283	162	13,42	46	8,28	30,24
B16-20	200501	122	201009	283	161	1,2	35	0,75	2,72
B17-20	200430	121	201009	283	162	24,96	15	15,41	56,24
B18-20	200429	120	201008	282	162	11,06	347	6,83	24,92
B19-20	200429	120	201008	282	162	1,34	348	0,83	3,03
BB0-20	200429	120	201008	282	162	1,21	305	0,75	2,74
Barc-20	200503	124	201010	284	160	5,23	90	3,27	11,94
Bor-20	200503	124	201012	286	162	17,35	185	10,71	39,09
Br1-20	191127	331	200327	86	120	0	270	0	0
Br1-20	200327	86	200813	226	140	1,57	137	1,12	4,08
Br1-20	200813	226	201125	330	104	0,94	298	0,9	3,3
Br2-19	191127	331	200327	86	120	5,68	159	4,74	17,29
Br2-20	200327	86	201125	330	244	0,96	127	0,39	1,44
Br3-20	200228	87	201125	330	243	14,86	142	6,11	22,32
Br5-19	190501	121	200328	87	331	255,97	185	77,33	282,27
Br7-20	200505	126	201009	283	157	48,62	174	30,97	113,04
Bru-20	200430	121	201008	282	161	14,48	19	8,99	32,82
Bud-20	200430	121	201008	282	161	18	10	11,18	40,81
D05-20	200502	123	201010	284	161	25,03	32	15,55	56,75
D07-20	200502	123	201010	284	161	30,66	22	19,04	69,51
D09-20	200502	123	201010	284	161	7,37	353	4,58	16,7
D12-20	200502	123	201010	284	161	1,47	10	0,91	3,32
E01-20	200429	120	201008	282	162	8,12	18	5,02	18,31
E02-20	200429	120	201008	282	162	22,41	6	13,83	50,5
E03-20	200429	120	201008	282	162	10,4	343	6,42	23,42
E04-20	200429	120	201008	282	162	1,86	6	1,15	4,19
E07-20	200429	120	201013	287	167	10,57	34	6,33	23,1
E08-20	200429	120	201013	287	167	4,02	13	2,41	8,78
E09-20	200429	120	201013	287	167	0,79	21	0,47	1,73
Fl01-20	200429	120	201008	282	162	16,14	132	9,96	36,37
G02-20	200502	123	201012	286	163	8,09	200	4,97	18,13
G03-20	200502	123	201012	286	163	3,21	193	1,97	7,18
G04-20	200502	123	201012	286	163	1,68	28	1,03	3,76
Go1-20	200503	124	201010	284	160	1,95	164	1,22	4,44
Haab-20	200503	124	201010	284	160	0,92	352	0,57	2,09
Hof01-20	200429	120	201008	282	162	11,5	179	7,1	25,92
K01-20	200503	124	201012	286	162	5,2	303	3,21	11,73
K02-20	200503	124	201012	286	162	12,59	297	7,77	28,36

K03-20	200503	124	201012	286	162	15,88	290	9,8	35,77
K04-20	200503	124	201012	286	162	20,76	291	12,81	46,76
K05-20	200503	124	201012	286	162	11,75	250	7,25	26,48
K06-20	200503	124	201010	284	160	2,69	111	1,68	6,13
K07-20	200503	124	201012	286	162	1,51	310	0,93	3,41
S01-20	200503	124	201010	284	160	1,07	225	0,67	2,44
S02-20	200503	124	201010	284	160	19,79	192	12,37	45,15
S04-20	200503	124	201010	284	160	28,57	206	17,86	65,17
S05-20	200503	124	201010	284	160	12,15	258	7,59	27,72
Ske02-20	200501	122	201010	284	162	134,64	225	83,11	303,35
Ske03-20	200501	122	201010	284	162	68,86	228	42,5	155,14
Ske04-20	200501	122	201010	284	162	30,64	231	18,91	69,03
Ske05-20	200501	122	201010	284	162	12,56	227	7,75	28,31
Skf00-20	200428	119	201008	282	163	5,06	32	3,1	11,32
Skf01-20	200428	119	201008	282	163	12,65	108	7,76	28,32
T01-20	200504	125	201012	286	161	3,99	285	2,48	9,05
T03-20	200504	125	201012	286	161	10,34	254	6,42	23,43
T04-20	200504	125	201012	286	161	11,7	240	7,27	26,52
T05-20	200504	125	201012	286	161	11,04	242	6,86	25,03
T06-20	200504	125	201012	286	161	11,05	234	6,86	25,06
T07-20	200504	125	201012	286	161	7,27	245	4,52	16,49
T08-20	200503	124	201010	284	160	1,38	271	0,86	3,15

Appendix E: Melt water runoff to selected rivers in summer 2020, derived from summer surface balance.

ΔS: area in a given elevation range where summer balance is negative, **∑ΔS**: cumulative area above a given elevation, **ΔQ_s**: melt water runoff from a given elevation range, **$\sum \Delta Q_s$** : cumulative melt water runoff from an area above given elevation.

Tungnaá water drainage basin

Elevation (m a. s. l.)		ΔS km^2	∑ΔS km^2	ΔQ_s $(10^6 m^3)$	$\sum \Delta Q_s$ $(10^6 m^3)$
1350	1400	0,3	0,3	0,4	0,4
1300	1350	6,0	6,4	8,1	8,5
1250	1300	10,0	16,3	15,5	24,0
1200	1250	10,9	27,2	20,1	44,0
1150	1200	9,5	36,7	22,8	66,8
1100	1150	11,4	48,1	33,9	100,7
1050	1100	10,8	58,9	37,2	137,9
1000	1050	9,5	68,4	35,9	173,8
950	1000	9,1	77,5	36,8	210,6
900	950	8,8	86,2	37,4	248,0
850	900	6,6	92,9	29,6	277,5
800	850	6,8	99,6	32,1	309,6
750	800	5,7	105,4	28,7	338,3
700	750	3,7	109,1	20,1	358,4
650	700	0,8	109,9	4,5	362,9

Sylgja water drainage basin

Elevation (m a. s. l.)		ΔS km^2	∑ΔS km^2	ΔQ_s $(10^6 m^3)$	$\sum \Delta Q_s$ $(10^6 m^3)$
1300	1350	1,1	1,1	1,5	1,5
1250	1300	3,4	4,5	5,3	6,8
1200	1250	5,5	10,0	10,2	17,0
1150	1200	8,2	18,2	18,4	35,4
1100	1150	5,8	24,0	16,2	51,6
1050	1100	6,2	30,2	20,7	72,3
1000	1050	5,8	36,0	23,0	95,2
950	1000	1,9	37,9	8,5	103,7
900	950	0,8	38,7	3,8	107,5
850	900	0,0	38,7	0,2	107,7

Western Skaftá cauldron water drainage basin

Elevation (m a. s. l.)		ΔS km^2	∑ΔS km^2	ΔQ_s $(10^6 m^3)$	$\sum \Delta Q_s$ $(10^6 m^3)$
1700	1750	2,2	2,2	0,7	0,7
1650	1700	7,2	9,4	2,7	3,3
1600	1650	7,9	17,3	3,7	7,1
1550	1600	5,1	22,4	2,8	9,9
1500	1550	2,6	25,1	1,6	11,5
1450	1500	0,0	25,1	0,0	11,5

Eastern Skaftár cauldron water drainage basin

Elevation (m a. s. l.)		ΔS km^2	∑ΔS km^2	ΔQ_s ($10^6 m^3$)	$\sum\Delta Q_s$ ($10^6 m^3$)
1750	1800	2,4	2,4	0,4	0,4
1700	1750	9,7	12,1	2,8	3,2
1650	1700	13,7	25,8	4,5	7,7
1600	1650	9,4	35,2	3,5	11,2
1550	1600	4,1	39,3	1,6	12,8

Grímsvötn water drainage basin

Elevation (m a. s. l.)		ΔS km^2	∑ΔS km^2	ΔQ_s ($10^6 m^3$)	$\sum\Delta Q_s$ ($10^6 m^3$)
1800	1850	0,3	0,3	0,0	0,0
1750	1800	4,6	4,9	1,0	1,0
1700	1750	23,8	28,7	7,5	8,5
1650	1700	48,6	77,2	16,2	24,7
1600	1650	30,9	108,1	12,8	37,5
1550	1600	20,0	128,1	12,5	50,0
1500	1550	16,6	144,8	18,2	68,2
1450	1500	9,7	154,5	13,8	82,0
1400	1450	13,8	168,3	21,6	103,6
1350	1400	1,5	169,8	2,2	105,8

Kaldakvísl water drainage basin

Elevation (m a. s. l.)		ΔS km^2	∑ΔS km^2	ΔQ_s ($10^6 m^3$)	$\sum\Delta Q_s$ ($10^6 m^3$)
1800	1850	1,9	1,9	0,1	0,1
1750	1800	7,1	9,0	0,7	0,8
1700	1750	20,2	29,2	5,0	5,8
1650	1700	16,8	46,0	7,8	13,6
1600	1650	14,4	60,4	9,0	22,6
1550	1600	18,5	78,9	14,4	37,0
1500	1550	24,0	103,0	22,4	59,5
1450	1500	28,0	130,9	30,2	89,7
1400	1450	22,4	153,4	27,4	117,1
1350	1400	20,8	174,1	30,5	147,5
1300	1350	20,2	194,3	37,1	184,6
1250	1300	21,1	215,4	45,3	229,9
1200	1250	20,4	235,8	50,6	280,5
1150	1200	19,3	255,1	56,1	336,6
1100	1150	17,3	272,4	58,0	394,6
1050	1100	16,1	288,5	60,2	454,9
1000	1050	14,1	302,6	57,8	512,7
950	1000	9,2	311,8	39,6	552,3
900	950	2,6	314,4	11,5	563,8

Jökulsá á Fjöllum water drainage basin

Elevation (m a. s. l.)		ΔS km^2	∑ΔS km^2	ΔQ_s ($10^6 m^3$)	$\sum\Delta Q_s$ ($10^6 m^3$)
1900	1950	0,0	0,0	0,0	0,0
1850	1900	4,9	5,0	0,3	0,3
1800	1850	17,0	22,0	1,6	1,9
1750	1800	21,8	43,8	4,0	5,9
1700	1750	39,1	82,9	10,6	16,6
1650	1700	80,5	163,4	25,9	42,4
1600	1650	122,3	285,7	47,7	90,1
1550	1600	100,7	386,4	55,2	145,3
1500	1550	93,3	479,6	60,6	205,9
1450	1500	80,0	559,6	61,9	267,8
1400	1450	69,0	628,6	63,7	331,5
1350	1400	54,7	683,3	60,6	392,1
1300	1350	43,2	726,5	56,5	448,6
1250	1300	46,8	773,3	71,9	520,5
1200	1250	49,8	823,1	90,9	611,4
1150	1200	49,6	872,7	111,4	722,8
1100	1150	43,8	916,5	116,4	839,2
1050	1100	31,3	947,8	97,2	936,4
1000	1050	31,4	979,2	109,6	1046,0
950	1000	29,1	1008,3	113,5	1159,5
900	950	24,4	1032,8	104,6	1264,1
850	900	21,1	1053,8	97,4	1361,5
800	850	18,7	1072,6	92,4	1453,9
750	800	12,3	1084,8	65,2	1519,1
700	750	3,7	1088,5	21,3	1540,4

Kreppa and Kverká water drainage basin

Elevation (m a. s. l.)		ΔS km^2	$\sum\Delta S$ km^2	ΔQ_s $(10^6 m^3)$	$\sum\Delta Q_s$ $(10^6 m^3)$
1850	1900	1,1	1,2	0,3	0,4
1800	1850	4,1	5,4	0,4	0,8
1750	1800	2,7	8,0	0,4	1,2
1700	1750	3,8	11,9	0,8	2,0
1650	1700	5,2	17,0	1,5	3,5
1600	1650	41,4	58,4	14,9	18,4
1550	1600	20,5	78,9	12,4	30,8
1500	1550	13,4	92,4	10,6	41,4
1450	1500	16,4	108,7	15,2	56,6
1400	1450	20,0	128,7	21,2	77,7
1350	1400	26,2	154,9	29,4	107,1
1300	1350	20,4	175,3	24,9	132,0
1250	1300	15,5	190,7	23,3	155,3
1200	1250	18,1	208,8	34,3	189,7
1150	1200	17,4	226,2	40,4	230,1
1100	1150	16,0	242,2	41,8	271,9
1050	1100	0,0	252,7	30,2	302,1
1000	1050	12,1	263,2	39,0	341,1
950	1000	13,3	272,4	48,9	390,0
900	950	12,6	279,5	50,6	440,6
850	900	12,6	284,9	53,4	494,0
800	850	10,4	287,7	46,0	540,0
750	800	7,3	288,2	34,8	574,8
700	750	3,5	288,2	18,5	593,3
650	700	0,4	288,2	2,5	595,8

Hálslón water drainage basin

Elevation (m a. s. l.)		ΔS km^2	$\sum\Delta S$ km^2	ΔQ_s $(10^6 m^3)$	$\sum\Delta Q_s$ $(10^6 m^3)$
1600	1650	11,4	11,4	5,4	5,4
1550	1600	33,1	44,5	22,4	27,8
1500	1550	65,3	109,8	55,9	83,7
1450	1500	70,0	179,9	65,0	148,7
1400	1450	99,0	278,8	87,5	236,2
1350	1400	133,7	412,6	138,3	374,5
1300	1350	130,3	542,9	151,6	526,1
1250	1300	123,4	666,3	173,7	699,9
1200	1250	98,2	764,5	166,3	866,2
1150	1200	82,2	846,7	167,3	1033,4
1100	1150	64,5	911,2	157,1	1190,5
1050	1100	55,1	966,3	156,4	1347,0
1000	1050	46,1	1012,4	149,1	1496,1
950	1000	39,4	1051,8	142,4	1638,5
900	950	31,6	1083,4	124,6	1763,2
850	900	26,8	1110,1	112,5	1875,7
800	850	25,1	1135,3	111,3	1987,0
750	800	25,2	1160,5	119,0	2105,9
700	750	22,4	1182,9	117,8	2223,7
650	700	12,1	1194,9	68,8	2292,5
600	650	1,1	1196,1	6,7	2299,2

Jökulsá á Fljótsdal water drainage basin

Elevation (m a. s. l.)		ΔS km^2	ΣΔS km^2	ΔQ_s ($10^6 m^3$)	$\Sigma\Delta Q_s$ ($10^6 m^3$)
1550	1600	0,0	0,0	0,0	0,0
1500	1550	0,1	0,1	0,1	0,1
1450	1500	1,1	1,2	1,0	1,1
1400	1450	2,1	3,4	2,0	3,0
1350	1400	3,1	6,5	3,3	6,3
1300	1350	5,9	12,4	7,1	13,4
1250	1300	16,1	28,5	22,4	35,8
1200	1250	15,8	44,3	24,2	60,0
1150	1200	17,0	61,3	30,4	90,4
1100	1150	14,3	75,6	31,3	121,7
1050	1100	11,9	87,6	32,6	154,3
1000	1050	11,1	98,6	36,6	191,0
950	1000	8,7	107,3	33,7	224,7
900	950	5,5	112,8	24,2	248,9
850	900	4,2	117,0	19,7	268,6
800	850	3,1	120,1	15,9	284,5
750	800	1,9	122,0	11,3	295,9
700	750	1,7	123,8	10,8	306,7
650	700	1,0	124,8	6,6	313,3

Hornafjarðarfljót water drainage basin

Elevation (m a. s. l.)		ΔS km^2	∑ΔS km^2	ΔQ_s ($10^6 m^3$)	$\sum\Delta Q_s$ ($10^6 m^3$)
1450	1500	1,2	1,2	1,0	1,0
1400	1450	8,2	9,4	6,3	7,4
1350	1400	12,7	22,2	11,7	19,1
1300	1350	19,2	41,4	21,0	40,0
1250	1300	37,9	79,3	49,7	89,7
1200	1250	28,8	108,1	40,4	130,1
1150	1200	20,3	128,4	31,5	161,7
1100	1150	18,9	147,3	32,8	194,4
1050	1100	14,2	161,5	28,1	222,5
1000	1050	11,1	172,5	24,3	246,7
950	1000	10,4	182,9	25,0	271,8
900	950	8,1	191,0	21,7	293,5
850	900	5,4	196,3	16,1	309,6
800	850	4,5	200,8	14,5	324,1
750	800	4,1	204,9	13,8	338,0
700	750	3,4	208,4	12,7	350,7
650	700	3,6	212,0	14,8	365,4
600	650	2,6	214,5	11,6	377,0
550	600	1,8	216,4	8,6	385,6
500	550	1,7	218,1	8,7	394,3
450	500	1,2	219,3	6,4	400,7
400	450	1,1	220,4	6,4	407,1
350	400	0,8	221,3	5,1	412,2
300	350	0,6	221,9	3,9	416,1
250	300	0,8	222,7	5,6	421,7
200	250	1,6	224,3	11,5	433,2
150	200	2,3	226,6	18,9	452,1
100	150	2,5	229,1	21,8	473,9
50	100	1,9	231,0	17,5	491,4
0	50	2,2	233,2	21,5	512,9

Jökulsá á Breiðamerkursandi water drainage basin

Elevation (m a. s. l.)		ΔS km^2	∑ΔS km^2	ΔQ_s ($10^6 m^3$)	$\sum\Delta Q_s$ ($10^6 m^3$)
1700	1750	1,0	1,0	0,2	0,2
1650	1700	4,2	5,2	1,4	1,6
1600	1650	14,2	19,5	6,3	8,0
1550	1600	19,0	38,5	11,8	19,8
1500	1550	22,9	61,4	19,4	39,2
1450	1500	36,1	97,5	33,2	72,4
1400	1450	51,2	148,7	51,4	123,7
1350	1400	83,5	232,2	100,2	224,0
1300	1350	83,4	315,6	123,3	347,3
1250	1300	51,7	367,3	95,4	442,7
1200	1250	34,7	401,9	74,0	516,7
1150	1200	28,3	430,3	66,7	583,5
1100	1150	23,8	454,0	60,2	643,7
1050	1100	20,4	474,4	55,5	699,2
1000	1050	17,5	492,0	50,9	750,0
950	1000	19,2	511,2	59,4	809,4
900	950	19,8	531,0	65,2	874,6
850	900	18,5	549,5	65,8	940,4
800	850	18,7	568,1	70,1	1010,5
750	800	19,9	588,1	80,5	1091,0
700	750	16,7	604,8	71,3	1162,3
650	700	27,3	632,0	121,6	1283,9
600	650	19,3	651,3	90,2	1374,1
550	600	19,0	670,3	96,1	1470,1
500	550	10,3	680,6	54,2	1524,3
450	500	5,1	685,7	27,8	1552,1
400	450	7,1	692,8	39,9	1592,0
350	400	5,0	697,8	28,9	1620,9
300	350	4,5	702,2	27,6	1648,5
250	300	5,3	707,6	35,9	1684,4
200	250	4,4	712,0	33,0	1717,4
150	200	5,0	717,0	40,9	1758,3
100	150	4,6	721,6	41,1	1799,4
50	100	3,8	725,5	37,4	1836,8
0	50	1,7	727,2	17,5	1854,4

Breiðárlón/Fjallsárlón water drainage basin

Elevation (m a. s. l.)		ΔS km^2	∑ΔS km^2	ΔQ_s ($10^6 m^3$)	$\sum\Delta Q_s$ ($10^6 m^3$)
1700	1750	0,0	0,0	0,0	0,0
1650	1700	0,4	0,4	0,0	0,0
1600	1650	3,6	4,0	1,0	1,1
1550	1600	4,3	8,3	2,7	3,8
1500	1550	5,8	14,1	4,9	8,7
1450	1500	5,0	19,0	4,9	13,6
1400	1450	5,3	24,3	6,1	19,7
1350	1400	6,4	30,7	9,1	28,8
1300	1350	12,9	43,6	19,4	48,1
1250	1300	6,2	49,8	11,1	59,2
1200	1250	5,8	55,6	12,3	71,5
1150	1200	4,8	60,3	11,4	82,9
1100	1150	4,5	64,8	11,7	94,6
1050	1100	5,0	69,8	13,4	108,0
1000	1050	6,1	75,9	17,3	125,3
950	1000	6,7	82,6	20,7	145,9
900	950	7,9	90,4	26,1	172,0
850	900	6,2	96,7	22,3	194,3
800	850	7,6	104,2	29,0	223,3
750	800	8,6	112,8	34,7	258,0
700	750	6,6	119,3	28,0	286,1
650	700	6,2	125,6	28,2	314,2
600	650	7,3	132,9	34,8	349,0
550	600	8,2	141,1	41,3	390,4
500	550	8,3	149,4	43,6	434,0
450	500	8,8	158,1	48,0	482,1
400	450	10,4	168,5	58,2	540,3
350	400	8,7	177,2	50,7	591,0
300	350	7,0	184,2	43,1	634,1
250	300	6,4	190,6	43,3	677,4
200	250	6,0	196,7	44,9	722,3
150	200	6,0	202,6	48,9	771,2
100	150	4,5	207,1	39,5	810,7
50	100	3,7	210,8	34,7	845,4
0	50	4,1	214,9	39,4	884,8

Skeiðarársandur (Gígja) water drainage basin

Elevation (m a. s. l.)		ΔS km^2	∑ΔS km^2	ΔQ_s ($10^6 m^3$)	$\sum\Delta Q_s$ ($10^6 m^3$)
1700	1750	1,9	1,9	0,4	0,4
1650	1700	21,5	23,5	6,6	7,1
1600	1650	82,0	105,5	32,2	39,3
1550	1600	86,0	191,5	51,9	91,1
1500	1550	110,8	302,3	89,6	180,7
1450	1500	106,5	408,8	93,7	274,4
1400	1450	104,2	513,0	99,4	373,9
1350	1400	91,4	604,4	96,2	470,0
1300	1350	77,9	682,4	90,5	560,6
1250	1300	69,6	751,9	90,0	650,6
1200	1250	60,5	812,4	88,1	738,6
1150	1200	54,6	867,0	89,5	828,2
1100	1150	51,4	918,4	94,8	923,0
1050	1100	46,3	964,8	102,0	1025,0
1000	1050	41,5	1006,3	106,9	1131,9
950	1000	40,3	1046,6	116,1	1248,0
900	950	37,2	1083,8	115,9	1363,9
850	900	38,6	1122,5	128,6	1492,5
800	850	32,6	1155,1	116,5	1609,0
750	800	27,3	1182,4	105,8	1714,8
700	750	25,2	1207,6	106,0	1820,8
650	700	20,2	1227,8	92,8	1913,6
600	650	15,5	1243,4	75,2	1988,8
550	600	23,3	1266,6	118,4	2107,2
500	550	20,5	1287,2	108,8	2216,1
450	500	13,5	1300,7	74,7	2290,8
400	450	12,0	1312,7	70,9	2361,6
350	400	13,0	1325,7	80,8	2442,5
300	350	14,1	1339,8	92,8	2535,3
250	300	12,2	1352,0	88,5	2623,7
200	250	12,1	1364,1	94,2	2717,9
150	200	11,2	1375,3	93,6	2811,6
100	150	9,8	1385,1	85,4	2897,0
50	100	6,0	1391,1	53,9	2950,9
0	50	2,4	1393,5	21,9	2972,8

Djúpá water drainage basin

Elevation (m a. s. l.)		ΔS km^2	∑ΔS km^2	ΔQ_s ($10^6 m^3$)	$\sum\Delta Q_s$ ($10^6 m^3$)
1450	1500	0,1	0,1	0,1	0,1
1400	1450	0,3	0,4	0,3	0,4
1350	1400	0,7	1,1	0,8	1,2
1300	1350	3,5	4,6	4,3	5,5
1250	1300	3,3	7,9	4,3	9,8
1200	1250	2,9	10,8	4,4	14,2
1150	1200	3,3	14,2	5,7	20,0
1100	1150	5,3	19,5	10,3	30,2
1050	1100	5,5	24,9	12,7	43,0
1000	1050	8,8	33,7	23,6	66,6
950	1000	7,4	41,1	23,2	89,8
900	950	7,4	48,5	26,2	116,0
850	900	6,3	54,8	24,2	140,2
800	850	6,6	61,4	28,4	168,5
750	800	6,0	67,4	29,7	198,2
700	750	3,5	70,9	19,1	217,3
650	700	2,5	73,4	14,1	231,4
600	650	0,6	74,0	3,6	235,0

Brunná water drainage basin

Elevation (m a. s. l.)		ΔS km^2	∑ΔS km^2	ΔQ_s ($10^6 m^3$)	$\sum\Delta Q_s$ ($10^6 m^3$)
1000	1050	0,8	0,8	2,3	2,3
950	1000	2,1	3,0	6,9	9,2
900	950	4,0	7,0	14,9	24,1
850	900	4,0	10,9	16,5	40,6
800	850	3,7	14,7	17,1	57,7
750	800	4,1	18,8	20,4	78,1
700	750	5,0	23,8	26,3	104,5
650	700	5,2	29,0	29,9	134,4
600	650	2,8	31,8	16,8	151,1

Hverfisfljót water drainage basin

Elevation (m a. s. l.)		ΔS km^2	∑ΔS km^2	ΔQ_s ($10^6 m^3$)	$\sum\Delta Q_s$ ($10^6 m^3$)
1700	1750	0,9	0,9	0,2	0,2
1650	1700	5,9	6,8	2,1	2,2
1600	1650	9,1	15,9	3,9	6,2
1550	1600	10,4	26,3	5,3	11,5
1500	1550	20,8	47,1	13,0	24,5
1450	1500	40,3	87,4	32,6	57,1
1400	1450	26,6	114,0	24,8	81,8
1350	1400	24,2	138,2	26,1	108,0
1300	1350	22,7	160,9	28,7	136,7
1250	1300	17,6	178,5	25,7	162,4
1200	1250	20,3	198,8	32,4	194,8
1150	1200	14,4	213,2	26,1	220,9
1100	1150	10,9	224,1	22,8	243,7
1050	1100	9,3	233,4	22,7	266,3
1000	1050	8,7	242,0	24,0	290,4
950	1000	8,6	250,6	27,6	317,9
900	950	7,9	258,5	28,9	346,8
850	900	7,8	266,3	31,4	378,3
800	850	6,8	273,1	30,2	408,5
750	800	8,5	281,6	41,5	450,0
700	750	10,7	292,2	56,8	506,8
650	700	11,2	303,4	63,9	570,8
600	650	6,0	309,4	35,9	606,6
550	600	0,2	309,6	1,1	607,7

Skaftá water drainage basin

Elevation (m a. s. l.)		ΔS km^2	∑ΔS km^2	ΔQ_s ($10^6 m^3$)	$\sum\Delta Q_s$ ($10^6 m^3$)
1650	1700	1,9	1,9	0,7	0,7
1600	1650	14,8	16,7	5,6	6,3
1550	1600	22,8	39,5	11,4	17,7
1500	1550	31,7	71,1	20,7	38,3
1450	1500	24,9	96,0	18,8	57,1
1400	1450	22,5	118,4	20,9	78,0
1350	1400	20,5	138,9	23,2	101,2
1300	1350	22,2	161,1	29,4	130,7
1250	1300	15,1	176,2	22,8	153,5
1200	1250	20,5	196,7	35,7	189,2
1150	1200	22,3	219,0	48,6	237,8
1100	1150	23,3	242,3	61,2	299,0
1050	1100	22,7	264,9	68,4	367,4
1000	1050	25,2	290,1	83,3	450,8
950	1000	20,2	310,3	73,3	524,0
900	950	16,8	327,1	65,8	589,8
850	900	13,5	340,6	56,2	646,0
800	850	14,2	354,8	63,7	709,7
750	800	12,4	367,2	60,8	770,5
700	750	9,9	377,1	52,1	822,6
650	700	6,3	383,4	34,3	856,9
600	650	0,8	384,2	4,6	861,6